Endogenous calcitonin gene-related peptide regulates lipid metabolism and energy homeostasis in male mice

Tian Liu[1], Akiko Kamiyoshi[1], Takayuki Sakurai[1], Yuka Ichikawa-Shindo[1], Hisaka Kawate[1], Lei Yang[1], Megumu Tanaka[1], Xian Xian[1], Akira Imai[1], Liuyu Zhai[1], Kazutaka Hirabayashi[1], Kun Dai[1], Keiya Tanimura[1], Teng Liu[1], Nanqi Cui[1], Kyoko Igarashi[2], Akihiro Yamauchi[2], Takayuki Shindo[1]

1. Department of Cardiovascular Research, Shinshu University Graduate School of Medicine, Nagano, Japan
2. Japan Bio Products Co., Ltd., Tokyo, Japan

Abbreviated title: CGRP regulates lipid metabolism

Key terms: Calcitonin gene-related peptide (CGRP), White adipose tissue (WAT), Lipolysis, Sympathetic nerve

Number of Figures: 8, **Table:** 1**, Supplementary Figures** 6

Address for correspondence
Akiko Kamiyoshi, PhD
Department of Cardiovascular Research
Shinshu University Graduate School of Medicine
Asahi 3-1-1, Matsumoto, Nagano, 390-8621, Japan
Tel: +81-263-37-2578
Fax: +81-263-37-3437
Email: organregen@shinshu-u.ac.jp

Disclosure statement: The authors have nothing to disclose

Abstract

Calcitonin gene-related peptide (CGRP) is a bioactive peptide produced by alternative splicing of the primary transcript of the calcitonin/CGRP gene. CGRP is largely distributed in the cardiovascular and nervous systems, where it acts as a regulatory factor. CGRP is also expressed in organs and tissues involved in metabolic regulation, including white adipose tissue (WAT), where its function is largely unknown. In this study, we examined the effects of endogenous CGRP on metabolic function. When we administered a high-fat diet to CGRP knockout (CGRP-/-) and wild-type (WT) mice for 10 weeks, we observed that food intake did not differ between the two groups, but body weight and visceral fat weight were significantly lower in CGRP-/- mice. Fatty liver changes were less severe in CGRP-/- mice, which also showed lower serum insulin and leptin levels. Glucose tolerance and insulin sensitivity were better in CGRP-/- than WT mice, and expired gas analysis revealed greater oxygen consumption by CGRP-/- mice. Adipocyte hypertrophy was suppressed in CGRP-/- mice, while expression of β3-adrenergic receptor, hormone-sensitive lipase and adiponectin was enhanced. Isoproterenol-induced glycerol release from WAT was higher in CGRP-/- than WT mice, and CGRP-/- mice showed elevated sympathetic nervous activity. β receptor-blockade canceled the beneficial effects of CGRP deletion on obesity. These results suggest that, in addition to its actions in the cardiovascular system, endogenous CGRP is a key regulator of metabolism and energy homeostasis *in vivo*.

Abbreviations

CGRP: Calcitonin gene-related peptide

AM: Adrenomedullin

CGRP-/-: CGRP knockout mice

WT: Wild-type mice

WAT: White adipose tissue

VO_2: Oxygen consumption

VCO_2: Carbon dioxide output

RER: Respiratory exchange ratio

Introduction

Calcitonin gene-related peptide (CGRP) is a 37-amino acid peptide produced by alternative splicing of the primary transcript of the calcitonin/CGRP gene (1). CGRP is expressed primarily in motor and sensory neurons in both the central and peripheral nervous systems and has been shown to exert a variety of effects within the cardiovascular system (2), including vasodilation and positive inotropic effects on the heart (3). CGRP is also widely distributed in the digestive tract, lungs, kidney, liver and adipose tissue (4,5), where it exerts various effects in addition to those affecting cardiovascular function (6-9). Associations between CGRP and human diseases, including hypertension (10), Raynaud's disease (11), coronary (12) and cerebral artery spasm (13) and migraine (14), have also been reported.

To investigate the pathophysiological actions of endogenous CGRP, we generated CGRP-specific knockout mice (CGRP-/-) using a targeting DNA construct that replaced exon 5, which encodes a CGRP-specific region of the gene (15). In these mice, only CGRP is deleted; levels of calcitonin expression remain normal. At a glance, CGRP-/- mice develop normally, with no obvious growth retardation or body mass change. However, closer observation reveals that blood pressure, heart rate and sympathetic nervous system activity are all higher in CGRP-/- than wild-type (WT) mice (15). CGRP-/- mice also show more severe damage in organ injury models, as CGRP modulates cytokine expression and prevents endothelial cell apoptosis (16) and fibrosis (17). More recently, we reported that endogenous CGRP protects against neointimal hyperplasia in a vascular injury model by suppressing vascular smooth muscle proliferation (18). These data clearly show that endogenous CGRP is an important mediator of organ homeostasis within the cardiovascular and nervous systems.

Based on its structural homology and similar vasodilatory effects, CGRP has been classified as an adrenomedullin (AM) family peptide. We and others recently reported that, in addition to its cardiovascular effects, AM is an important regulator of

metabolism (19,20), and CGRP appears to similarly contribute to metabolic regulation. For example, CGRP is reportedly involved in regulating glucose metabolism (21), insulin sensitivity (22) and appetite (23). Interestingly, an earlier report showed that levels of CGRP are elevated in obese humans (24,25) and animals (26), and it was suggested that CGRP may contribute to metabolic diseases as it does to cardiovascular diseases. However, the pathophysiological importance of CGRP to metabolic disease remains unclear. In the present study, therefore, we investigated the function of endogenous CGRP in the metabolic system by chronically challenging WT and CGRP-/- mice with a high-fat diet and analyzing the phenotypes that emerge.

Materials and methods

Animals

CGRP and calcitonin are encoded by the same gene. To avoid the effects of calcitonin deficiency, we generated CGRP-/- mice using a targeting DNA construct that replaced exon 5 of the gene, which encodes a CGRP-specific region (15). C57BL/6 pure background male mice were used. The mice were maintained under specific pathogen-free conditions in an environmentally controlled (12-h light, 12-h dark cycle; room temperature, 22 ± 2 °C) room. All experiments were performed at the Division of Laboratory Animal Research, Department of Life Science, Research Center for Human and Environmental Sciences, Shinshu University. All animal experiments were conducted in accordance with the ethical guidelines of Shinshu University.

Measurement of food intake

Mice were kept on either on normal diet (4.7% energy as fat) or high-fat diet (32% energy as fat) fat (Clea Japan, Inc., Tokyo, Japan). To measure food intake, mice were housed separately in regular cages with a food intake measuring device (Shinfactory, Fukuoka, Japan). After allowing the mice to acclimate for at least 24 h, food intake was measured over a period of 24 h.

Expired gas analysis

Expired gas was analyzed using a Columbus Instruments Oxymax system (Columbus Instruments, Columbus, OH). Mice were housed individually in plastic chambers with unlimited access to food and water. After allowing the mice to acclimate to the chambers for 48 h, measurements were begun. O_2 consumption (VO_2), CO_2 output (VCO_2), respiratory exchange ratio (RER) and energy expenditure were recorded every 10 min for 48 h under a 12-h light-dark cycle at a room temperature of 22 ± 2 °C.

RNA extraction and quantitative real-time RT-PCR

Total RNA was extracted from tissues using TRIZOL Reagent (Invitrogen, Carlsbad, CA), after which the sample was treated with DNA-Free (Ambion, Austin, TX) to remove contaminating DNA and subjected to reverse transcription using a High Capacity cDNA Reverse Transcription Kit (Applied Biosystems, Carlsbad, CA). Quantitative real-time RT-PCR was carried out using an Applied Biosystems 7300 real time PCR System (Applied Biosystems) with SYBR green (Toyobo, Osaka, Japan) or Realtime PCR Master Mix (Toyobo). Values were normalized to mouse GAPDH (Pre-Developed TaqMan assay reagents, Applied Biosystems). Primers are listed in Table 1.

Glucose and insulin tolerance tests

For the oral glucose tolerance test (OGTT), mice were fasted for 16 h and then fed 1 g/kg glucose (Wako, Tokyo, Japan). Blood glucose was measured 0, 15, 30, 60 and 120 min after the glucose load. Serum insulin concentrations were measured using an enzyme-linked immunosorbent assay (ELISA) kit (Shibayagei, Gunma, Japan). For the insulin tolerance test (ITT), mice were fasted for 2 h, after which 1.5 U/kg human insulin (Humulin R, Eli Lilly Japan, Hyogo, Japan) was injected intraperitoneally. Blood glucose was then measured 0, 15, 30, 60 and 120 min after the injection.

Histology

White adipose tissue (WAT) and the liver were excised from each mouse, fixed in 4% paraformaldehyde for 24 h and embedded in paraffin. The tissues were then cut into 5-μm sections, which were stained with hematoxylin-eosin (HE) and/or Masson trichrome (MT). For F4/80 immunohistochemical analysis, sections were incubated with rat anti-mouse F4/80 antibody (Thermo Fisher Scientific, Waltham, MA). The distribution of adipocyte sizes was evaluated using BIOREVO BZ-9000 BZ-H1

measurement software (KEYENCE, Osaka, Japan).

Urinary catecholamine levels

To determine the urinary levels of a norepinephrine metabolite, normetanephrine, mice were housed in individual metabolic cages. After 3 days, a small amount of 6 N HCl was added to the beaker placed in the cage, and the acidic urine was collected for the next 24 h. Urinary normetanephrine concentrations were then measured by a subcontractor (SRL, Tokyo, Japan).

Open field test

The apparatus consisted of an empty bright open-field arena surrounded by walls (45 x 45 x 40 cm). Twice each day, mice were individually placed in the center of the apparatus, which initiated a 10-min test session. Mouse behavior was recorded and analyzed using a SMART (Spontaneous Motor Activity Recording & Tracking) v. 3.0 software system (Panlab, Barcelona, Spain).

Primary adipocyte lipolysis activity

Equal amounts of epididymal WAT from WT and CGRP-/- mice were incubated in DMEM containing 2% fatty acid-free BSA and 10 μM isoproterenol. The tissue was incubated for 3 h at 37°C under a 5% CO_2 atmosphere, during which 10 μl of medium were extracted at 1-h intervals. The collected samples were incubated for 5 min at 37°C after adding free glycerol reagent. The absorbance at 540 nm was then measured and compared to absorbances obtained with glycerol standard solutions.

Western blotting

Mice were fasted overnight and injected 1.25 U/kg insulin or saline via the tail vein. Five minutes after the injection, WAT was excised, lysed in ice-cold RIPA Lysis Buffer

System (Santa Cruz Biotechnology, Dallas, TX) supplemented with PosSTOP phosphatase inhibitor (Roche Applied Science, Penzberg, Germany) and then sonicated. The resultant lysates were subjected to electrophoresis using TGX gel (Bio-Rad), transferred to PVDF membranes (Bio-Rad) and probed using antibodies against AMPK, phospho-AMPK (p-AMPK, Thr^{172}), HSL and phospho-HSL (p-HSL, Ser^{563}) (Cell Signaling Technology, Danvers, MA). Anti-β-tubulin antibody (Santa Cruz Biotechnology) served as a loading control. The bound antibodies were visualized using chemiluminescent HRP substrate (Merck Millipore, Billerica, MA), and the chemiluminescence was analyzed using an Image Quant LAS 4000 system (GE Healthcare, Little Chalfont, UK).

β blocker administration.

Propranolol (AstraZeneca, London, UK), a non-selective β-adrenergic receptor antagonist was dissolved in 0.5% methylcellulose. CGRP-/- mice on a high-fat diet were orally administered either propranolol (30 mg/kg/day) or control vehicle in their drinking water for 8 weeks, beginning when they were 8 weeks old. Body weights were measured weekly.

Statistical analysis

Values are expressed as means ± SEM. Student's t test, two-way ANOVA or Chi-squared test was used to determine significant differences. For the analysis of energy expenditure, we used ANCOVA analysis (27). All analyses were performed using SPSS software (v.18). Values of $P < 0.05$ were considered significant.

Results

CGRP-/- mice show resistance to weight gain without a change of appetite

We initially explored changes in the body weights of WT and CGRP-/- mice on normal and high-fat diets. The body weights of the mice were measured weekly for 10 weeks. When on a normal diet (4.7% energy as fat), the two groups exhibited similar weight gains from 8 to 18 weeks of age. CGRP-/- mice tended to have lower body weights than WT mice, but the difference was not significant (Fig. 1A). On a high-fat diet (32% energy as fat), both WT and CGRP-/- mice had higher body weights than mice on a normal diet, but the weight gains were clearly smaller in CGRP-/- than WT mice (Fig. 1B).

The difference in weight gain did not appear to reflect a difference in appetite or food intake, which were similar in WT and CGRP-/- mice on a high-fat (Fig. 2B) or normal diet (Fig. 2A). Furthermore, quantitative real-time PCR analysis of expression of several key orexigenic (neuropeptide Y (NPY) and agouti-related protein (AgRP)) and anorexigenic (pro-opiomelanocortin (POMC) and cocaine-amphetamine-related transcript (CART)) neuropeptides in the hypothalami of WT and CGRP-/- mice on a high-fat diet revealed no significant difference (Fig. 2C).

CGRP-/- mice showed elevated O_2 consumption

To gain information about general energy metabolism, we analyzed the expired gas from WT and CGRP-/- mice on normal diet (Fig. 3A-D) and high-fat diet (Fig. 3E-H). When fed a normal diet, CGRP-/- mice showed higher VO_2 and VCO_2 than WT mice (Fig. 3A and B). On a high-fat diet, the difference became even more apparent, with CGRP-/- mice exhibiting markedly higher VO_2 and VCO_2 than WT mice (Fig. 3E and F). There was no significant difference in the respiratory exchange ratio (RER) (Fig. 3C, G). Energy expenditure showed tendency of higher levels in CGRP-/- mice,

whether on a normal (Fig. 3D) or high-fat diet (Fig. 3H). CGRP-/- showed significantly higher energy expenditure/lean body mass under high fat diet (Supplementary Figure 1).

Glucose metabolism was enhanced in CGRP-/- mice

Because CGRP-/- mice resisted weight gain and showed changes in the expired gas, we next evaluated glucose and other metabolic parameters in WT and CGRP-/- mice after 10 weeks of high-fat diet. CGRP-/- mice showed better tolerance to a glucose load. This was apparent at nearly all time points tested during oral glucose tolerance tests (OGTT; Fig. 4A). Combined with the results of insulin tolerance tests (ITT; Fig. 4B), these data show that glucose metabolism was enhanced in CGRP-/- mice. On the other hand, the OGTT and ITT results were not significantly different between WT and CGRP-/- on normal diet (Supplementary Fig. 2), suggesting that the enhanced glucose metabolism in CGRP-/- becomes apparent only under the high-fat diet. Consistent with their resistance to body weight gains, the serum concentrations of insulin and the adipocyte-derived hormone leptin were significantly lower in CGRP-/- than WT mice (Fig. 4C and D). On the other hand, serum concentrations of triglyceride (TG), free fatty acid (FFA) and total cholesterol (TC) were similar in the two groups (Fig. 4E). These results demonstrate that glucose tolerance and insulin handling are enhanced in CGRP-/- mice on a high-fat diet, as compared to WT mice on the same diet.

Adipocyte hypertrophy and fatty liver changes were suppressed in CGRP-/- mice

Consistent with their resistance to weight gain while on a high-fat diet, CGRP-/- mice had less white adipose tissue (WAT) than WT mice (Fig. 5A). CGRP-/- also showed lower lean body mass weight after the high-fat diet (Fig. 5B). Analysis of the size distribution of adipocytes in WAT revealed that they skewed toward smaller sizes in CGRP-/- mice (upper panel of Fig. 5C and Fig. 5D). In obesity, adipocyte hypertrophy is accompanied by chronic adipose inflammation. In WT mice, the WAT

was infiltrated by large numbers of macrophages, but this infiltration was suppressed in CGRP-/- mice (lower panel of Fig. 5C).

The high-fat diet also resulted in development of a fatty liver. However, liver weights were significantly lower in CGRP-/- than WT mice (Fig. 5E), with fewer lipid-containing vacuoles (Fig. 5F upper panel). In addition, Masson trichrome staining showed that fibrotic changes at perivascular lesions were also suppressed in CGRP-/- mice (Fig. 5F lower panel).

Upregulated expression of lipolysis-related genes in WAT from CGRP-/- mice on a high-fat diet

To further examine the mechanism underlying the resistance to adipocyte hypertrophy and obesity in CGRP-/- mice, we used quantitative real-time PCR to assess gene expression in WAT from mice fed a high-fat diet for 10 weeks. We found that expression of genes associated with lipolysis, including hormone-sensitive lipase (HSL), comparative gene identification-58 (CGI-58), perilipin and β3-adrenergic receptor (β3AR), were all significantly upregulated in CGRP-/- mice. In particular, levels of β3AR expression were increased several-fold as compared to WT mice (Fig. 6A). The expression of adiponectin (Fig. 6B) and peroxisome proliferator-activated receptors (PPARs) (Fig. 6C) was also significantly elevated in CGRP-/- mice, which may account for the smaller, well-functioning adipocytes in CGRP-/- WAT, even in mice on the high-fat diet. Interestingly, expression of mitochondria-related genes, including mitochondrial transcription factor A (TFAM), estrogen related receptor alpha (ERRα) and cytochrome C oxidase (COX IV), was significantly higher in CGRP-/- than WT mice (Fig. 6D). Similarly, expression of several lipolysis and mitochondria-related genes was also significantly upregulated in WAT from mice fed a normal diet (Supplementary Fig. 3).

The expressions of brown adipose tissue (BAT) markers in BAT and beige-ing

associated genes in WAT were not different between WT and CGRP-/- (Supplementary Fig. 4), suggesting that the metabolic alteration in CGRP-/- mice could mainly be attributed to WAT, but not to either BAT or beige adipose tissue.

HSL plays the central role in lipolysis in WAT, and activation of AMP-activated protein kinase (AMPK) can modulate adipocyte metabolism by upregulating pathways that favor energy dissipation versus lipid storage in WAT. We used Western blotting to examine phosphorylation of HSL on Ser563 and AMPK on Thr172. Phosphorylation of HSL and AMPK showed tendency of elevation in WAT from CGRP-/- mice (Fig. 6E, F).

These results collectively suggest that lipolysis is elevated in CGRP-/- mice, which may explain the resistance to adipocyte hypertrophy and obesity.

Ability to release glycerol is preserved in CGRP-/- mice on a high-fat diet

We next examined the ability of WAT from WT and CGRP-/- mice to release glycerol *in vitro*. Epididymal WAT was collected from mice and incubated in culture medium containing 10 μM isoproterenol. Glycerol released into the medium was then measured at 1 h intervals for 3 h. In WT mice, the ability to release glycerol was significantly reduced by a high-fat diet as compared to a normal diet (Fig. 7 left). On the other hand, glycerol release was preserved in CGRP-/- mice, even on the high-fat diet. (Fig. 7 right).

Elevated sympathetic nerve activity and locomotor activity in CGRP-/- mice

CGRP is known to contribute to the regulation of cardiovascular function through inhibitory modulation of sympathetic nervous activity (15). To assess sympathetic nerve activity of WT and CGRP-/- mice, we measured urinary levels of normetanephrine, a catecholamine metabolite, and found that normetanephrine excretion was significantly higher in CGRP-/- than WT mice (Fig. 8A). This suggests that sympathetic nervous

activity is augmented in CGRP-/- mice.

We assessed locomotor activity by placing mice in the center of an empty bright open field arena surrounded by walls. Recording their movement for 10 min revealed that CGRP-/- mice traveled significantly longer distance than WT mice (Fig. 8B). Apparently, CGRP-/- mice are more active than WT mice.

We tested whether the body weight difference between WT and CGRP-/- mice could be canceled by suppressing the elevation in sympathetic nervous activity. When propranolol, a non-selective β blocker, was administered during the high-fat diet, the body weight difference between WT and CGRP-/- mice disappeared (Fig. 8C). The significant differences in VO_2 and VCO_2 on the high-fat diet were also canceled by the β blocker (Supplementary Fig. 5). We also analyzed the gene expression in WAT from mice fed a high-fat diet with oral administration of the β blocker, and found that the difference between CGRP-/- and WT was canceled by the β blocker (Supplementary Fig. 6).

Discussion

Our main findings in this study are that CGRP-/- mice are protected from high-fat diet-induced obesity and display improved glucose handling and insulin sensitivity. CGRP-/- mice also showed elevated oxygen consumption and carbon dioxide output. Consistent with the resistance to weight gain, CGRP-/- mice had less fat mass and lower liver weights than WT mice, with less adipocyte hypertrophy and fatty liver changes than WT mice. In the WAT from CGRP-/- mice, expression of genes related to lipolysis and mitochondria was elevated, and glycerol release was preserved, even in mice on a high-fat diet. In addition, sympathetic nerve activity and locomotor activity were both elevated in CGRP-/- mice. These findings clearly show that endogenous CGRP plays pivotal roles in metabolic regulation.

Using a different knockout mouse line, Walker et al. also reported that while on a high-fat diet, CGRP-/- mice had lower body weights than WT mice (5). Focusing on metabolic changes in the liver and skeletal muscle, they observed increased hepatic activity of the β-oxidation marker 3-hydroxyacyl coenzyme A dehydrogenase in CGRP-/- mice fed a high-fat diet, and lower expression and activation of acetyl coenzyme A carboxylase, an enzyme involved in lipogenesis. In CGRP-/- skeletal muscle, activation of AMPK was elevated, as was the activity of the mitochondrial marker citrate synthase. However, because obesity involves enlargement of visceral fat and chronic adipose inflammation, in this study, we focused on changes in WAT. CGRP-/- mice showed suppressed adipocyte hypertrophy and macrophage infiltration. Thus expression levels of genes associated with lipolysis and adipocyte differentiation as well as mitochondria-related genes were all significantly elevated in CGRP-/- WAT. In addition, HSL and AMPK, which promote lipolysis and energy dissipation in WAT (28), were also more activate in CGRP-/- WAT.

CGRP is expressed in sensory C and Aδ-fibers via activation of transient receptor potential vanilloid 1 (TRPV1) (29). Interestingly, the phenotype of TRPV1 knockout

mice (TRPV1-/-) resembles that of CGRP-/- mice, in that TRPV1-/- mice are also protected from diet-induced obesity (30). On an 11% fat diet, TRPV1-/- mice gained significantly less adiposity than WT mice, despite equivalent energy intake. The precise mechanism by which TRPV1 influences energy and lipid handling is unclear, but it has been suggested that TRPV1 contributes to the regulation of adipocyte function. TRPV1 triggers release of neuropeptides from sensory nerve terminals innervating fatty tissues (30). This suggests the resistance to obesity and adiposity exhibited by TRPV1-/- mice could be, at least in part, explained by decreased release of CGRP.

Our results differ from those of Danaher et al., who reported that exogenous administration of CGRP evoked lipolysis through elevation of fatty-acid β-oxidation and AMPK signaling both *in vitro* and *in vivo* (31). It may be that effects of exogenous CGRP administration do not reflect the physiologically significant effects on metabolic processes revealed by manipulating endogenous CGRP. Carter et al. reported that CGRP-expressing neurons in the outer external lateral subdivision of the parabrachial nucleus, which project to the laterocapsular division of the central nucleus of the amygdala, form a functionally important circuit for suppressing appetite (23). Lutz et al. reported that intracerebroventricular injection of CGRP(8-37), a CGRP antagonist, increased food intake (32). These findings suggest CGRP exerts anorectic effects within the central nervous system. However, because CGRP is produced by various tissues other than central nervous system and functions as a circulating hormone as well as a neurotransmitter, the CGRP-/- mouse is a suitable model for evaluating the total effect of endogenous CGRP on food-intake. Walker et al. reported that food intake was increased in CGRP-/- mice on a high-fat diet (5). In the present study, by contrast, we detected no difference of food-intake between CGRP-/- and WT mice, whether on a high-fat or normal diet. We also confirmed that there was no difference in hypothalamic levels of orexigenic or anorexigenic neuropeptides between the two groups. A key difference between the present study and that of Walker et al. was the high-fat diet

389 regimen. Those investigators observed increased food intake only by CGRP-/- mice on
390 a 60% fat diet, whereas our high-fat diet contained 32% fat. In addition, they analyzed
391 total food-intake during a study period of 42-224 days, whereas we evaluated daily
392 food-intake for 10 weeks. Thus both the content and feeding period differed between
393 the two studies, which could affect the phenotype of CGRP-/- mice. Consistent with that
394 idea, Walker et al. reported severe fatty liver changes with serum alanine transaminase
395 (ALT) levels of up to 300 U/L in WT mice and 100 U/L in CGRP-/- mice (5). In our
396 model, by contrast, ALT was elevated to about 80 U/L in both groups (data not shown).
397 Although the metabolic functions of CGRP have been reported, its role in insulin
398 sensitivity remains controversial, and previous studies ascribed both pro- and
399 anti-diabetic actions to CGRP (33). In streptozotocin-induced diabetic rats, for example,
400 CGRP-immunoreactive nerves were markedly increased in the epidermis and dermis
401 from an early stage, implicating altered in CGRP in the initial stages of diabetes (34).
402 Leighton et al. reported that CGRP is a potent inhibitor of both basal and
403 insulin-stimulated rates of glycogen synthesis in skeletal muscle *in vitro* (22), while
404 Molina et al. reported that intravenous infusion of CGRP caused insulin resistance *in*
405 *vivo* (35). On the other hand, Sun et al. reported that intramuscular transfer of CGRP
406 gene suppressed pro-inflammatory Th1 subsets and promoted anti-inflammatory Th2
407 subsets, which ameliorated β cell destruction in streptozotocin-induced diabetes (36). In
408 the present study, we found that CGRP deletion reduced hyperinsulinemia and
409 improved glucose tolerance and insulin sensitivity in mice on a high-fat diet. These
410 results suggest endogenous CGRP exerts negative metabolic effects in obesity.
411 The loss of CGRP's effect on sympathetic nerve activity may also contribute to
412 the metabolic changes seen in CGRP-/- mice. We previously reported that CGRP-/-
413 mice showed elevated blood pressures and heart rates, and suggested that CGRP acts to
414 inhibit sympathetic effects on cardiovascular function (15). In the present study, we
415 observed that urinary normetanephrine excretion was increased in CGRP-/- mice, which

also displayed hyperactivity in an open field test. These observations are consistent with the idea that sympathetic nervous activity is increased in CGRP-/- mice. It is thus noteworthy that propranolol, a β blocker that inhibits sympathetic nerve activity, eliminated the difference in weight gain between WT and CGRP-/- mice on high-fat diet. The significant differences in VO_2, VCO_2 and the gene expression in WAT on the high-fat diet were also canceled by β blocker. We therefore also suggest that CGRP contributes to the regulation of metabolism through inhibitory modulation of sympathetic nervous activity.

At a glance, our results suggest CGRP blockade could be useful in the treatment of obesity; however, its varied effects in multiple organs and tissues may make its use complicated. Very recently, Nilsson et al. reported that a long acting (half-life >10 h) CGRP analogue improved metabolic conditions in ob/ob mice and diet-induced obese rats (37). In the future, studies using conditional or inducible gene-edited mice may help further our understanding of the pathophysiological functions of CGRP in metabolic diseases and provide novel therapeutic approaches targeting this attractive molecule.

In summary, we found that CGRP-/- mice were protected from high-fat diet-induced obesity and displayed enhanced glucose metabolism. In CGRP-/- mice, adipocyte hypertrophy was suppressed by elevated lipolysis and sympathetic nervous activity. Our findings clearly show that endogenous CGRP is a key regulator of metabolism, and could be a novel therapeutic target in metabolic and cardiovascular diseases.

Declaration of interest

None.

Funding

This study was supported by Grants-in-Aid for Scientific Research (KAKENHI); Core Research for Evolutionary Science and Technology (CREST) of Japan Science and Technology Agency (JST) and the Japan Agency for Medical Research and Development (AMED); National Cardiovascular Center research grant for cardiovascular diseases; Grants-in aid of The Public Trust Fund For Clinical Cancer Research; Mitsui Life Social Welfare Foundation; Takeda Science Foundation research grant; Opto-Science and Technology research grant; Takeda Medical Research Foundation grant; Elderly Eye Disease Research Foundation grant; Novartis Foundation for Gerontological Research grant; Research grant from the Cosmetology Research Foundation; SENSHIN Medical Research Foundation; Kanzawa Medical Research Foundation; Ono Medical Research Foundation; Nagao Memorial Fund; Nakatomi Foundation; Japan Vascular Disease Research Foundation; YOKOYAMA Foundation for Clinical Pharmacology; and Banyu Life Science Foundation International.

References

1. Rosenfeld MG, Mermod JJ, Amara SG, Swanson LW, Sawchenko PE, Rivier J, Vale WW, Evans RM. Production of a novel neuropeptide encoded by the calcitonin gene via tissue-specific RNA processing. Nature 1983; 304:129-135
2. Holzer P. Local effector functions of capsaicin-sensitive sensory nerve endings: involvement of tachykinins, calcitonin gene-related peptide and other neuropeptides. Neuroscience 1988; 24:739-768
3. Wimalawansa SJ. Calcitonin gene-related peptide and its receptors: molecular genetics, physiology, pathophysiology, and therapeutic potentials. Endocr Rev 1996; 17:533-585
4. Brain SD, Williams TJ, Tippins JR, Morris HR, MacIntyre I. Calcitonin gene-related peptide is a potent vasodilator. Nature 1985; 313:54-56
5. Walker CS, Li X, Whiting L, Glyn-Jones S, Zhang S, Hickey AJ, Sewell MA, Ruggiero K, Phillips AR, Kraegen EW, Hay DL, Cooper GJ, Loomes KM. Mice lacking the neuropeptide alpha-calcitonin gene-related peptide are protected against diet-induced obesity. Endocrinology 2010; 151:4257-4269
6. Hughes JJ, Levine AS, Morley JE, Gosnell BA, Silvis SE. Intraventricular calcitonin gene-related peptide inhibits gastric acid secretion. Peptides 1984; 5:665-667
7. Sala C, Andreose JS, Fumagalli G, Lomo T. Calcitonin gene-related peptide: possible role in formation and maintenance of neuromuscular junctions. J Neurosci 1995; 15:520-528
8. Harzenetter MD, Novotny AR, Gais P, Molina CA, Altmayr F, Holzmann B. Negative regulation of TLR responses by the neuropeptide CGRP is mediated by the transcriptional repressor ICER. J Immunol 2007; 179:607-615
9. Fisher LA, Kikkawa DO, Rivier JE, Amara SG, Evans RM, Rosenfeld MG, Vale WW, Brown MR. Stimulation of noradrenergic sympathetic outflow by calcitonin gene-related peptide. Nature 1983; 305:534-536
10. Edvinsson L, Ekman R, Thulin T. Reduced levels of calcitonin gene-related peptide (CGRP) but not substance P during and after treatment of severe hypertension in man. J Hum Hypertens 1989; 3:267-270
11. Bunker CB, Terenghi G, Springall DR, Polak JM, Dowd PM. Deficiency of calcitonin gene-related peptide in Raynaud's phenomenon. Lancet 1990; 336:1530-1533
12. McEwan J, Larkin S, Davies G, Chierchia S, Brown M, Stevenson J, MacIntyre I, Maseri A. Calcitonin gene-related peptide: a potent dilator of human epicardial coronary arteries. Circulation 1986; 74:1243-1247
13. Juul R, Hara H, Gisvold SE, Brubakk AO, Fredriksen TA, Waldemar G, Schmidt JF, Ekman R, Edvinsson L. Alterations in perivascular dilatory neuropeptides (CGRP, SP, VIP) in the external jugular vein and in the

cerebrospinal fluid following subarachnoid haemorrhage in man. Acta Neurochir (Wien) 1995; 132:32-41

14. Karsan N, Goadsby PJ. Calcitonin gene-related peptide and migraine. Curr Opin Neurol 2015; 28:250-254

15. Oh-hashi Y, Shindo T, Kurihara Y, Imai T, Wang Y, Morita H, Imai Y, Kayaba Y, Nishimatsu H, Suematsu Y, Hirata Y, Yazaki Y, Nagai R, Kuwaki T, Kurihara H. Elevated sympathetic nervous activity in mice deficient in alphaCGRP. Circ Res 2001; 89:983-990

16. Kamiyoshi A, Sakurai T, Ichikawa-Shindo Y, Fukuchi J, Kawate H, Muto S, Tagawa Y, Shindo T. Endogenous alphaCGRP protects against concanavalin A-induced hepatitis in mice. Biochem Biophys Res Commun 2006; 343:152-158

17. Kamiyoshi A, Sakurai T, Ichikawa-Shindo Y, Iinuma N, Kawate H, Yoshizawa T, Koyama T, Muto S, Shindo T. Endogenous alpha-calcitonin gene-related peptide mitigates liver fibrosis in chronic hepatitis induced by repeated administration of concanavalin A. Liver Int 2009; 29:642-649

18. Yang L, Sakurai T, Kamiyoshi A, Ichikawa-Shindo Y, Kawate H, Yoshizawa T, Koyama T, Iesato Y, Uetake R, Yamauchi A, Tanaka M, Toriyama Y, Igarashi K, Shindo T. Endogenous CGRP protects against neointimal hyperplasia following wire-induced vascular injury. J Mol Cell Cardiol 2013; 59:55-66

19. Yoshizawa T, Sakurai T, Kamiyoshi A, Ichikawa-Shindo Y, Kawate H, Iesato Y, Koyama T, Uetake R, Yang L, Yamauchi A, Tanaka M, Toriyama Y, Igarashi K, Nakada T, Kashihara T, Yamada M, Kawakami H, Nakanishi H, Taguchi R, Nakanishi T, Akazawa H, Shindo T. Novel regulation of cardiac metabolism and homeostasis by the adrenomedullin-receptor activity-modifying protein 2 system. Hypertension 2013; 61:341-351

20. Iemura-Inaba C, Nishikimi T, Akimoto K, Yoshihara F, Minamino N, Matsuoka H. Role of adrenomedullin system in lipid metabolism and its signaling mechanism in cultured adipocytes. Am J Physiol Regul Integr Comp Physiol 2008; 295:R1376-1384

21. Rossetti L, Farrace S, Choi SB, Giaccari A, Sloan L, Frontoni S, Katz MS. Multiple metabolic effects of CGRP in conscious rats: role of glycogen synthase and phosphorylase. Am J Physiol 1993; 264:E1-10

22. Leighton B, Cooper GJ. Pancreatic amylin and calcitonin gene-related peptide cause resistance to insulin in skeletal muscle in vitro. Nature 1988; 335:632-635

23. Carter ME, Soden ME, Zweifel LS, Palmiter RD. Genetic identification of a neural circuit that suppresses appetite. Nature 2013; 503:111-114

24. Zelissen PM, Koppeschaar HP, Lips CJ, Hackeng WH. Calcitonin gene-related peptide in human obesity. Peptides 1991; 12:861-863

25. Recober A, Goadsby PJ. Calcitonin gene-related peptide: A molecular link between obesity and migraine? Drug News Perspect 2010; 23:112-117

26. Gram DX, Hansen AJ, Wilken M, Elm T, Svendsen O, Carr RD, Ahren B,

Brand CL. Plasma calcitonin gene-related peptide is increased prior to obesity, and sensory nerve desensitization by capsaicin improves oral glucose tolerance in obese Zucker rats. Eur J Endocrinol 2005; 153:963-969

27. Tschop MH, Speakman JR, Arch JR, Auwerx J, Bruning JC, Chan L, Eckel RH, Farese RV, Jr., Galgani JE, Hambly C, Herman MA, Horvath TL, Kahn BB, Kozma SC, Maratos-Flier E, Muller TD, Munzberg H, Pfluger PT, Plum L, Reitman ML, Rahmouni K, Shulman GI, Thomas G, Kahn CR, Ravussin E. A guide to analysis of mouse energy metabolism. Nat Methods 2011; 9:57-63

28. Gaidhu MP, Fediuc S, Anthony NM, So M, Mirpourian M, Perry RL, Ceddia RB. Prolonged AICAR-induced AMP-kinase activation promotes energy dissipation in white adipocytes: novel mechanisms integrating HSL and ATGL. J Lipid Res 2009; 50:704-715

29. Zygmunt PM, Petersson J, Andersson DA, Chuang H, Sorgard M, Di Marzo V, Julius D, Hogestatt ED. Vanilloid receptors on sensory nerves mediate the vasodilator action of anandamide. Nature 1999; 400:452-457

30. Motter AL, Ahern GP. TRPV1-null mice are protected from diet-induced obesity. FEBS Lett 2008; 582:2257-2262

31. Danaher RN, Loomes KM, Leonard BL, Whiting L, Hay DL, Xu LY, Kraegen EW, Phillips AR, Cooper GJ. Evidence that alpha-calcitonin gene-related peptide is a neurohormone that controls systemic lipid availability and utilization. Endocrinology 2008; 149:154-160

32. Lutz TA, Rossi R, Althaus J, Del Prete E, Scharrer E. Evidence for a physiological role of central calcitonin gene-related peptide (CGRP) receptors in the control of food intake in rats. Neurosci Lett 1997; 230:159-162

33. Russell FA, King R, Smillie SJ, Kodji X, Brain SD. Calcitonin gene-related peptide: physiology and pathophysiology. Physiol Rev 2014; 94:1099-1142

34. Karanth SS, Springall DR, Francavilla S, Mirrlees DJ, Polak JM. Early increase in CGRP- and VIP-immunoreactive nerves in the skin of streptozotocin-induced diabetic rats. Histochemistry 1990; 94:659-666

35. Molina JM, Cooper GJ, Leighton B, Olefsky JM. Induction of insulin resistance in vivo by amylin and calcitonin gene-related peptide. Diabetes 1990; 39:260-265

36. Sun W, Wang L, Zhang Z, Chen M, Wang X. Intramuscular transfer of naked calcitonin gene-related peptide gene prevents autoimmune diabetes induced by multiple low-dose streptozotocin in C57BL mice. Eur J Immunol 2003; 33:233-242

37. Nilsson C, Hansen TK, Rosenquist C, Hartmann B, Kodra JT, Lau JF, Clausen TR, Raun K, Sams A. Long acting analogue of the calcitonin gene-related peptide induces positive metabolic effects and secretion of the glucagon-like peptide-1. Eur J Pharmacol 2016; 773:24-31

Figure Legends

Figure 1. Comparison of body weights between WT and CGRP-/- mice on a normal diet (4.7% energy as fat) (**A**) and high-fat diet (32% energy as fat) (**B**) from 8 to 18 weeks of age. n = 5 in both groups. Body weights were measured weekly and expressed as the mean ± SEM. Statistical significance was analyzed using two-way ANOVA. ***P<0.001. Experiments were repeated 4 times and similar results were obtained each time.

Figure 2. Food intake and levels of hypothalamic neuropeptides regulating appetite did not differ between CGRP-/- and WT mice. **A, B** Comparison of food intake per day between WT and CGRP-/- mice on either a normal diet (**A**) or high-fat diet (**B**). n = 5 in each group. Bars are the mean ± SEM. **C,** Quantitative real-time PCR analysis showing expression of the key hypothalamic orexigenic (neuropeptide Y (NPY) and agoutirelated protein (AgRP)) and anorexigenic (pro-opiomelanocortin (POMC) and cocaine-amphetamine-related transcript (CART)) neuropeptides in WT and CGRP-/- mice on a high-fat diet. n = 15 in each group. All values are expressed as mean ± SEM.

Figure 3. Expired gas analysis in WT and CGRP-/- mice on normal diet (**A**-**D**) or high-fat diet (**E**-**H**). Studies were performed under a 12-h light and 12-h dark cycle at a room temperature of 22 ± 2 °C. Oxygen consumption (VO_2) (**A**, **E**)**,** CO_2 production (VCO_2) (**B**, **F**), respiratory exchange ratio (RER) (**C**, **G**), and energy expenditure (**D**, **H**) were compared between WT and CGRP-/- mice. Means of these parameters for all day and the light and dark portions of the day are shown. n = 5 in each group. All values are expressed as the mean ± SEM. *P<0.05, **P<0.01, ***P<0.001 vs. WT.

Figure 4. Analysis of metabolism in WT and CGRP-/- mice after 10 weeks on a high-fat diet. **A, B,** Mice were subjected to oral glucose tolerance tests (OGTT) (**A**) and

insulin tolerance tests (ITT) (**B**) after 10 weeks on a high-fat diet. Area under the curve (AUC) data of OGTT and ITT were also calculated. For OGTT, 1 g/kg glucose was administered after fasting 16 h. For ITT, 1.5 U/kg insulin was intraperitoneally injected after fasting for 2 h. n = 5 in each group. All values are expressed as the mean ± SEM. Statistical significance was analyzed using repeated-measures ANOVA. *P<0.05. **C, D,** Serum insulin concentration (**C**) and leptin levels (**D**) after fasting overnight. n = 5 in each group. Bars depict means ± SEM. Statistical significance was analyzed using unpaired Student's t test. *P <0.05, **P <0.01. **E,** Serum level of triglyceride (TG), free fatty acid (FFA) and total cholesterol (TC) after fasting overnight. n = 5 in each group. Bars depict means ± SEM.

Figure 5. Pathological analysis of WT and CGRP-/- mice after 10 weeks of a high-fat diet. **A,** Comparison of weights of epididymal, mesenteric, perirenal and subcutaneous white adipose tissue (WAT) between WT and CGRP-/- mice. n = 5 in each group. *P<0.05. **B,** Comparison of body weight, lean body mass weight and fat mass weight between WT and CGRP-/- mice. Data are shown as the ratio between WT and CGRP-/- mice, and WT was assigned a value of 1. n = 5 in each group. **P<0.01, **P<0.001 vs. WT. **C,** Hematoxylin-eosin (HE) staining and F4/80 immunostaining of WAT sections. Scale bars = 100 μm. **D,** Adipocyte size distribution in sections of epididymal WAT. n = 5 in each group. All values are expressed as a percentage ± SEM. ***P<0.001 vs. WT using Chi-squared test. **E,** Comparison of liver weights between WT and CGRP-/- mice after high-fat diet. **F,** HE (upper panel) and Masson trichrome (MT) (lower panel) stained liver samples from WT and CGRP-/- mice. Scale bars = 100 μm.

Figure 6. Elevation of lipolysis-related factors in WAT from CGRP-/- mice on a high-fat diet. **A-D,** Expression of genes associated with lipolysis (**A**), adiponectin (**B**), and adipocyte differentiation (**C**), and mitochondria-related genes (**D**) in WAT. WT and

CGRP-/- mice were fed a high-fat diet for 10 weeks. n = 5 in each group. Expression levels in CGRP-/- were normalized to WT, which was assigned a value of 1. β3AR: β3-adrenergic receptor, HSL: hormone-sensitive lipase, CGI-58: comparative gene identification-58, AdPLA2: adipose phospholipase A2, PPAR: peroxisome proliferator activated receptor, TFAM: mitochondrial transcription factor A, ERRα: estrogen related receptor alpha, COX IV: cytochrome C oxidase, UCP: uncoupling protein. All values are expressed as the mean ± SEM. Statistical significance was analyzed using unpaired Student's t test. *P< 0.05, ** P < 0.01 vs. WT. **E,** Phosphorylation of AMP kinase (p-AMPK) (upper panels) and HSL (p-HSL) (lower panel) was analyzed in WAT from mice on a high-fat diet for 10 weeks. WAT was extracted and processed for Western blot analysis. β-tubulin was used as a loading control. Blots are representative of 3 experiments. **F,** Result of the densitometry analysis of the Western blotting. Bars depict means ± SEM.

Figure 7. Preserved lipolysis in WAT of CGRP-/- mice on a high-fat diet. WAT was excised from WT (left) and CGRP-/- (right) mice on a high-fat or normal diet for 10 weeks. Glycerol release from the excised WAT was measured *in vitro* by adding 10 μM isoproterenol at 1 h intervals for 3 h. n = 5 in each group. ** P <0.01 vs. WT.

Figure 8. Sympathetic nervous activity was elevated in CGRP-/- mice. **A,** Urinary catecholamine (normetanephrine) excretion in mice on a normal diet was significantly higher in CGRP-/- than WT mice. n =12 in each group. Bars depict means ± SEM. Statistical significance was analyzed using unpaired Student's t test. *P <0.05 vs. WT. **B,** Open field test comparing the activity levels of CGRP-/- and WT mice after 10 weeks on a high-fat diet. Shown is the total distance traveled in 10 min in during open field tests. n =12 in each group. Bars depict means ± SEM. Statistical significance was analyzed using unpaired Student's t test. **P <0.01 vs. WT. **C,** Comparison of body

660 weight between WT and CGRP-/- mice on a high-fat diet with oral administration of a β
661 blocker (propranolol). The data of CGRP-/- mice administered control vehicle is also
662 shown.

Table 1. Primers used for quantitative real-time PCR

Gene	Primer	
POMC	Forward	TGCCGAGATTCTGCTACAG
	Reverse	TGCTGCTGTTCCTGGGGC
CART	Forward	CCCGAGCCCTGGACATCTA
	Reverse	GCTTCGATCTGCAACATAGCG
NPY	Forward	ATGCTAGGTAACAAGCGAATG
	Reverse	TGTCGCAGAGCGGAGTAGTAT
AgRP	Forward	TGTGTAAGCTGCACGAGTC
	Reverse	GGCAGTAGCAAAAGGCATTG
β3AR	Forward	CAGTCCCTGCCTATGTTG
	Reverse	TTCCTGGATTCCTFCTCT
HSL	Forward	TCACGCTACATAAAGGCTCGT
	Reverse	CCACCCGTAAAGAGGGAACT
CGI58	Forward	CTACCTGGTGTCCCACGTCT
	Reverse	CAAGACCTCCTCCAAAACCA
Perilipin	Forward	CATCTCTACCCGCCTTCGAA
	Reverse	TGCTTGCAATGGGCACACT
AdPLA2	Forward	ATAACAGTCTTTCCTGGCTGGCCT
	Reverse	TCCATTTCTGTGTACCCAGGCTGT
Adiponectin	Forward	AGGTTGGATGGCAGGC
	Reverse	GTCTCACCCTTAGGACCAAGAA
PPARα	Forward	GGGATTGTGCACGTGCTTAA
	Reverse	TTTGGGAAGAGGAAGGTGTCA
PPARγ	Forward	CCCAATGGTTGCTGATTACAAA
	Reverse	AATAATAAGGTGGAGATGCAGGTTCT
PPARδ	Forward	CCACAACGCACCCTTTGTC
	Reverse	CCACACCAGGCCCTTCTCT
TFAM	Forward	GCTTGCTAAGATGATAGGATTCGT
	Reverse	TCGTCCAACTTCAGCCATCTG
ERRα	Forward	GTACTGCAGAGTGTGTGGATGGA
	Reverse	TCTAGGACCAGGTCCTCAGCAA
COX IV	Forward	GGTGGCCATCGAGACCAA
	Reverse	GGCGGAGAAGCCCTGAAT
UCP2	Forward	GCGCCAGATGAGCTTTGC
	Reverse	CCTTGGTGTAGAACTGTTTGACAGA
UCP3	Forward	AACGCTCCCCTAGGCAGGTA
	Reverse	CCCTCCTGAGCCACCATCT
UCP1	Forward	CCCTGGCAAAAACAGAAGGA
	Reverse	CCACACCAGGCCCCTTCTCT
PGC-1α	Forward	GGCACGCAGCCCTATTCA
	Reverse	CGACACGGAGAGTTAAAGGAAGA
CIDEA	Forward	AAACCATGACCGAAGTAGCC
	Reverse	AGGCCAGTTGTGATGACTAAGAC
PKDM16	Forward	CAGCACGGTGAAGCCATTC
	Reverse	GCGTGCATCGCTTGTG
Cox7α1	Forward	AAAGTGCTGCACGTCCTTG
	Reverse	TTCTCTGCCACACGGTTTTC
D2	Forward	GATGCTCCCAATTCCAGTGT
	Reverse	TGAACCAAAGTTGACCACCA

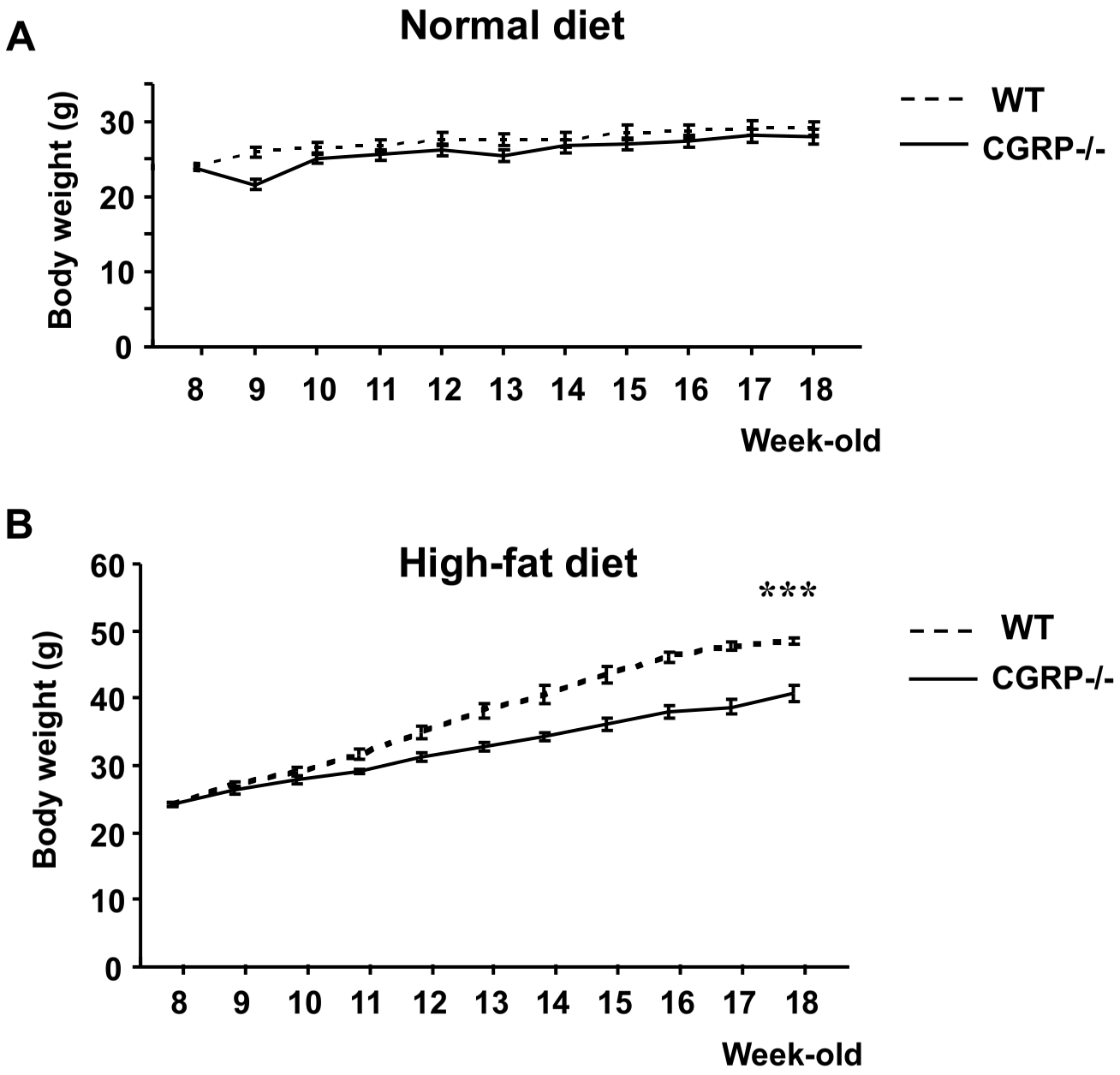
A
Normal diet
Body weight (g)
0
10
20
30
8
9
10
11
12
13
14
15
16
17
18
Week-old
WT
CGRP-/-
B
High-fat diet
***
Body weight (g)
0
10
20
30
40
50
60
8
9
10
11
12
13
14
15
16
17
18
Week-old
WT
CGRP-/-

Figure 1

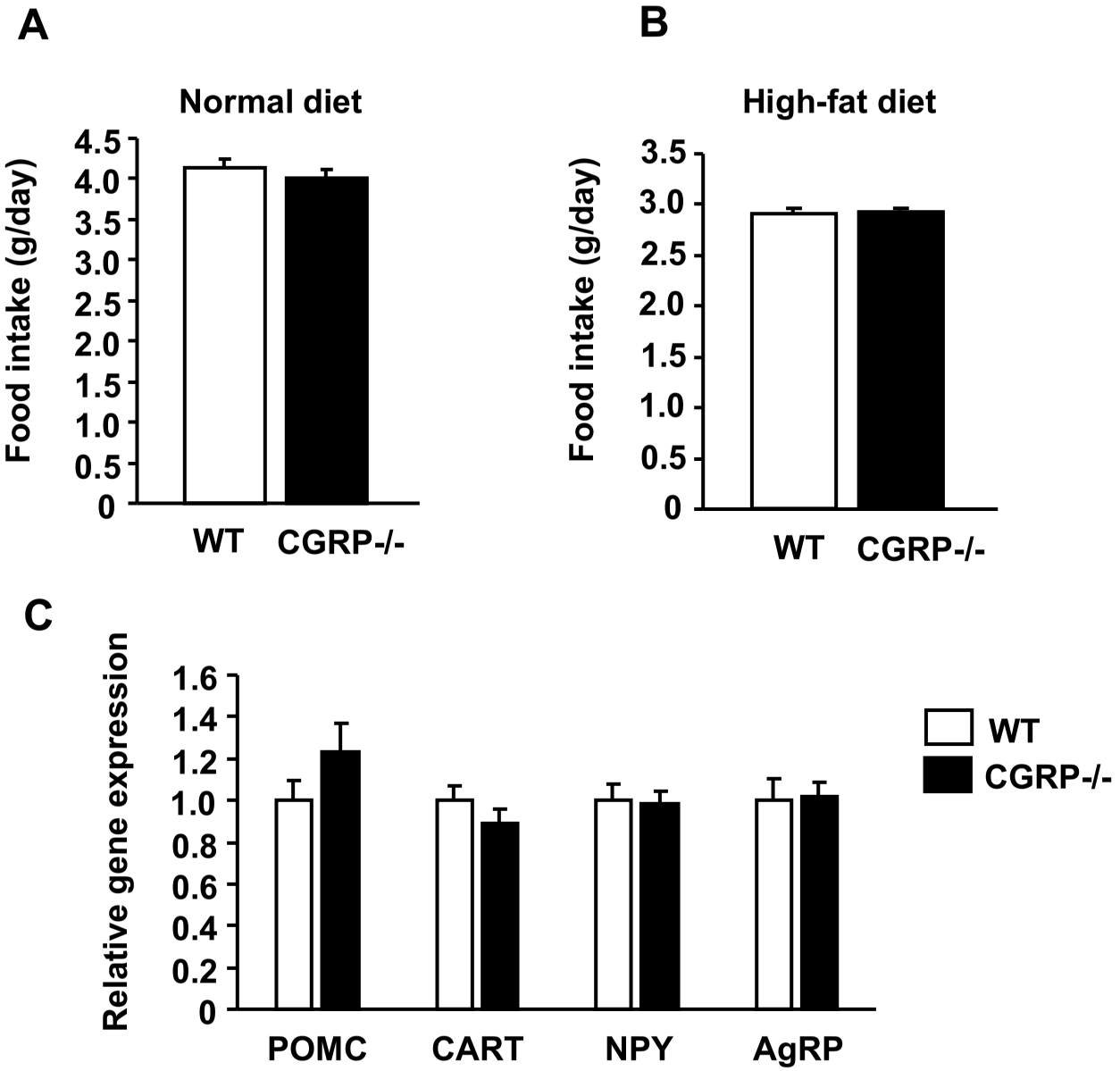
A
Normal diet
Food intake (g/day)
4.5
4.0
3.5
3.0
2.5
2.0
1.5
1.0
0.5
0
WT
CGRP-/-
B
High-fat diet
Food intake (g/day)
3.5
3.0
2.5
2.0
1.5
1.0
0.5
0
WT
CGRP-/-
C
Relative gene expression
1.6
1.4
1.2
1.0
0.8
0.6
0.4
0.2
0
POMC
CART
NPY
AgRP
WT
CGRP-/-

Figure 2

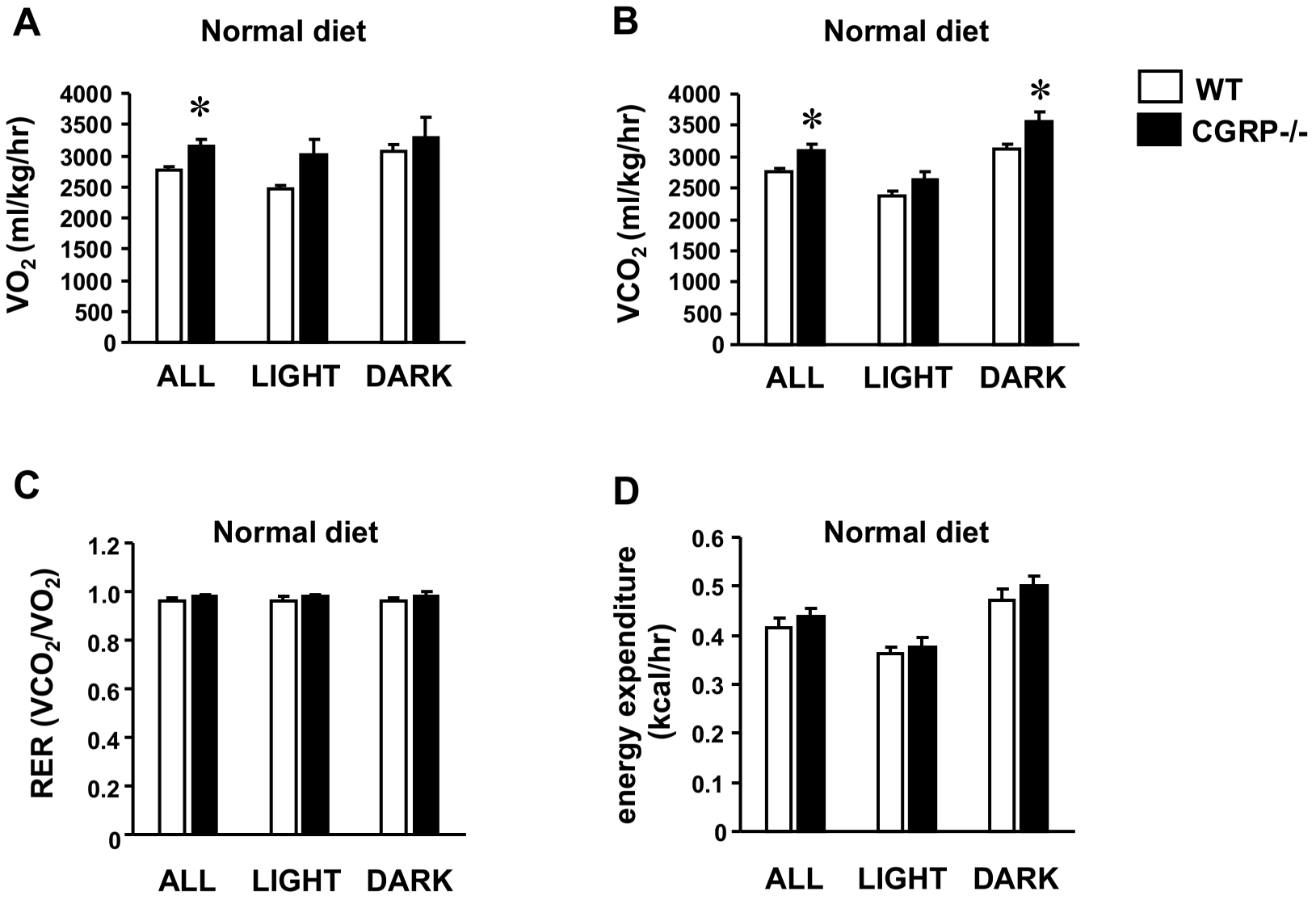
A
Normal diet
VO_2 (ml/kg/hr)
4000
3500
3000
2500
2000
1500
1000
500
0
*
ALL
LIGHT
DARK
B
Normal diet
VCO_2 (ml/kg/hr)
4000
3500
3000
2500
2000
1500
1000
500
0
*
*
ALL
LIGHT
DARK
WT
CGRP-/-
C
Normal diet
RER (VCO_2/VO_2)
1.2
1.0
0.8
0.6
0.4
0.2
0
ALL
LIGHT
DARK
D
Normal diet
energy expenditure (kcal/hr)
0.6
0.5
0.4
0.3
0.2
0.1
0
ALL
LIGHT
DARK

Figure 3

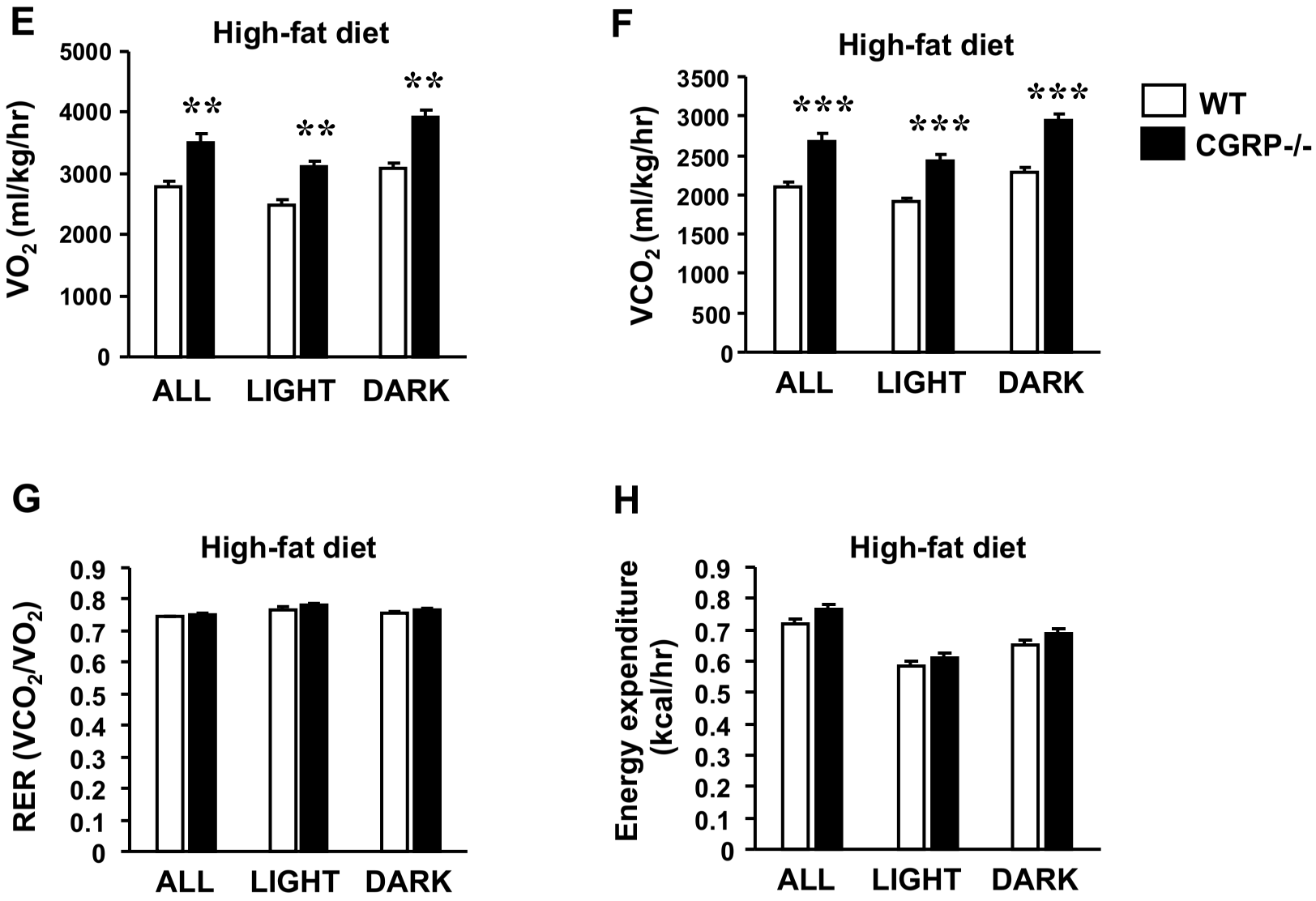
E
High-fat diet
VO_2 (ml/kg/hr)
5000
4000
3000
2000
1000
0
**
**
**
ALL
LIGHT
DARK
F
High-fat diet
VCO_2 (ml/kg/hr)
3500
3000
2500
2000
1500
1000
500
0
***
***
***
ALL
LIGHT
DARK
WT
CGRP-/-
G
High-fat diet
RER (VCO_2/VO_2)
0.9
0.8
0.7
0.6
0.5
0.4
0.3
0.2
0.1
0
ALL
LIGHT
DARK
H
High-fat diet
Energy expenditure (kcal/hr)
0.9
0.8
0.7
0.6
0.5
0.4
0.3
0.2
0.1
0
ALL
LIGHT
DARK

Figure 3

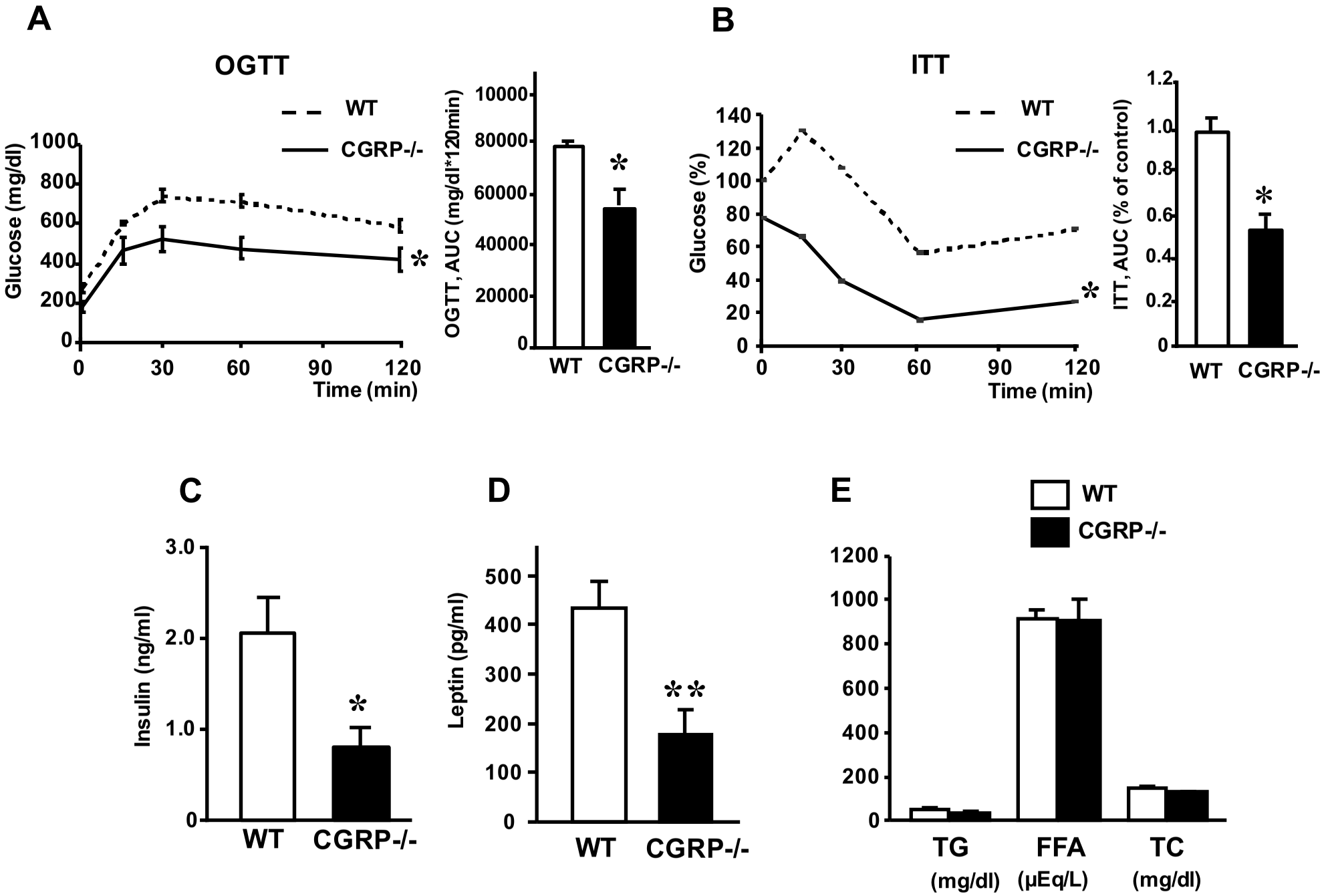
A
OGTT
WT
CGRP-/-
Glucose (mg/dl)
1000
800
600
400
200
0
0
30
60
90
120
Time (min)
*
OGTT, AUC (mg/dl*120min)
10000
80000
60000
40000
20000
0
*
WT
CGRP-/-
B
ITT
WT
CGRP-/-
Glucose (%)
140
120
100
80
60
40
20
0
0
30
60
90
120
Time (min)
*
ITT, AUC (% of control)
1.2
1.0
0.8
0.6
0.4
0.2
0
*
WT
CGRP-/-
C
Insulin (ng/ml)
3.0
2.0
1.0
0
*
WT
CGRP-/-
D
Leptin (pg/ml)
500
400
300
200
100
0
**
WT
CGRP-/-
E
WT
CGRP-/-
1200
1000
800
600
400
200
0
TG
(mg/dl)
FFA
(μEq/L)
TC
(mg/dl)

Figure 4

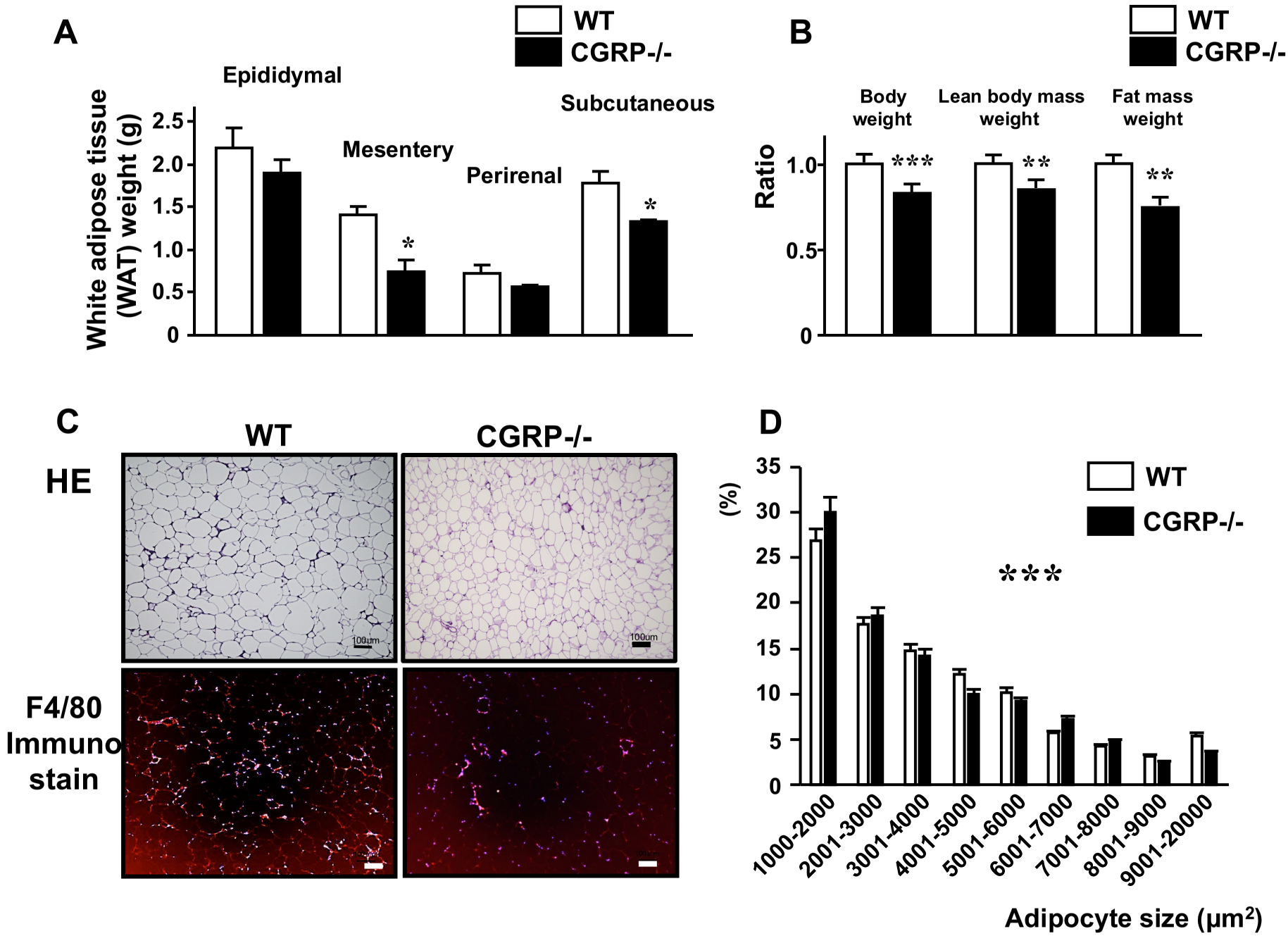
A
WT
CGRP-/-
Epididymal
Subcutaneous
Mesentery
Perirenal
White adipose tissue (WAT) weight (g)
2.5
2.0
1.5
1.0
0.5
0
*
*
B
WT
CGRP-/-
Body weight
Lean body mass weight
Fat mass weight
Ratio
1.0
0.5
0
***
**
**
C
WT
CGRP-/-
HE
F4/80 Immuno stain
100um
100um
D
WT
CGRP-/-
(%)
35
30
25
20
15
10
5
0
***
1000-2000
2001-3000
3001-4000
4001-5000
5001-6000
6001-7000
7001-8000
8001-9000
9001-20000
Adipocyte size (μm²)

Figure 5

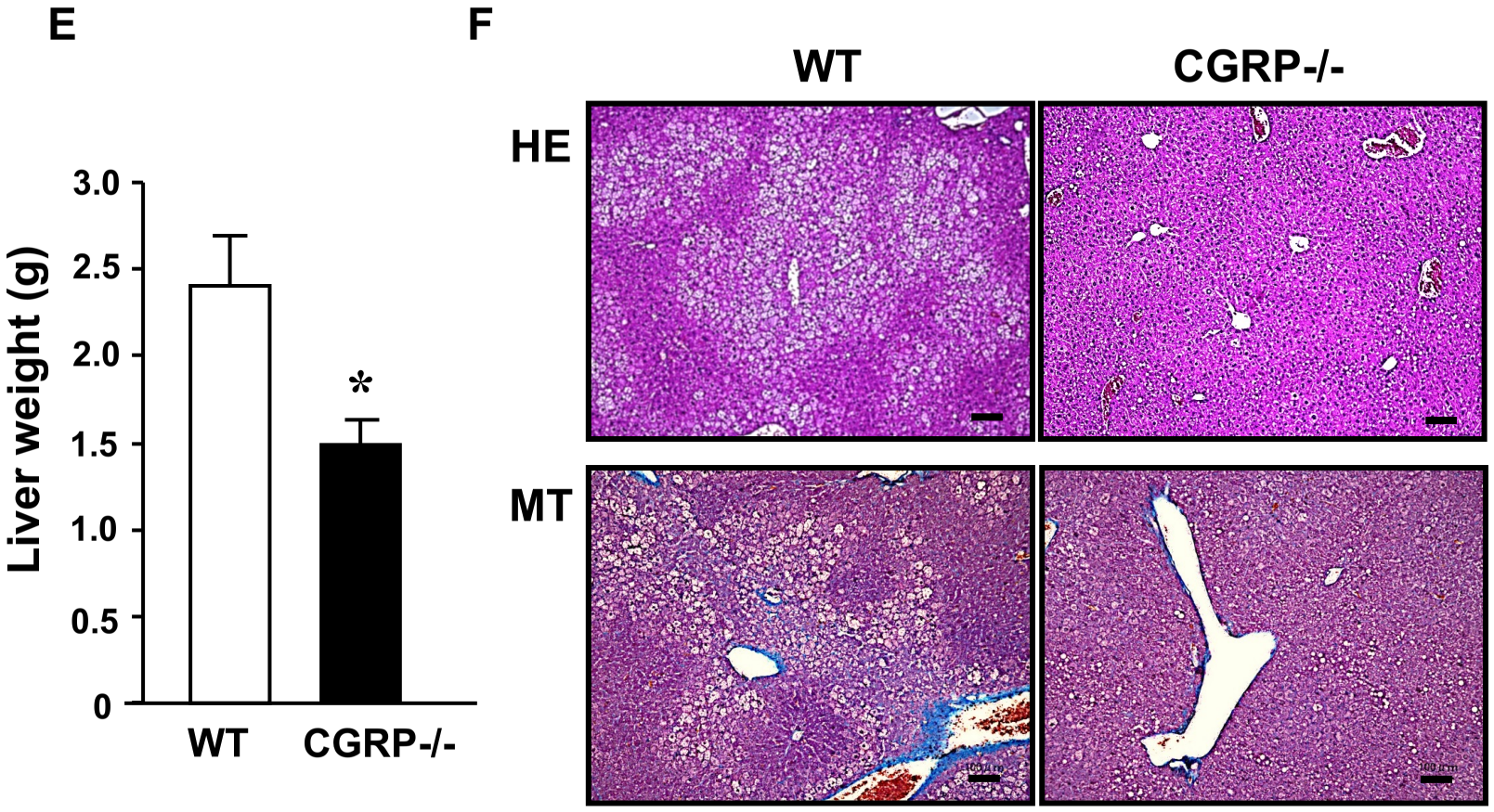

Figure 5

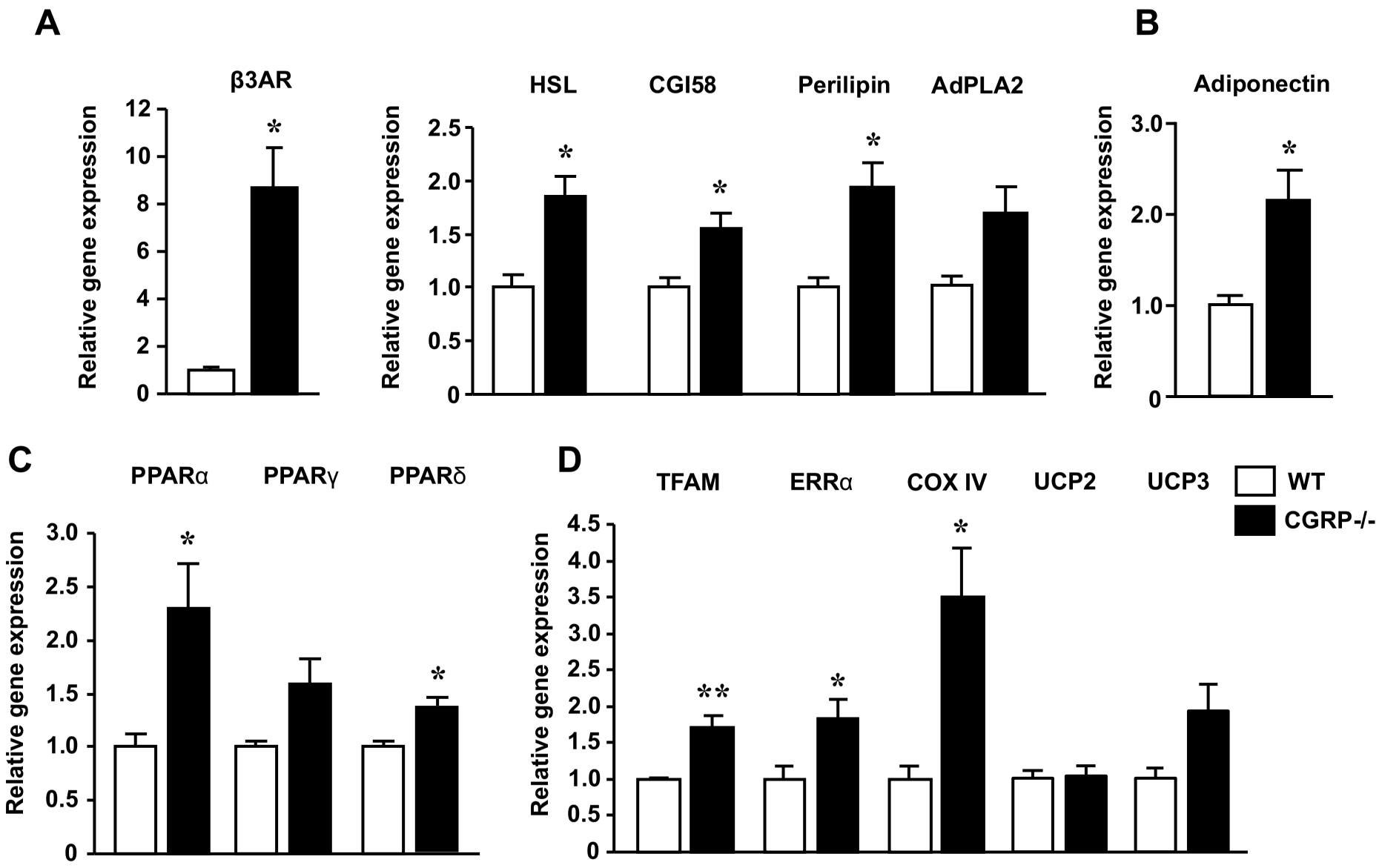
A
β3AR
Relative gene expression
12
10
8
6
4
2
0
*
HSL
CGI58
Perilipin
AdPLA2
Relative gene expression
2.5
2.0
1.5
1.0
0.5
0
*
*
*
B
Adiponectin
Relative gene expression
3.0
2.0
1.0
0
*
C
PPARα
PPARγ
PPARδ
Relative gene expression
3.0
2.5
2.0
1.5
1.0
0.5
0
*
*
D
TFAM
ERRα
COX IV
UCP2
UCP3
Relative gene expression
4.5
4.0
3.5
3.0
2.5
2.0
1.5
1.0
0.5
0
**
*
*
WT
CGRP-/-

Figure 6

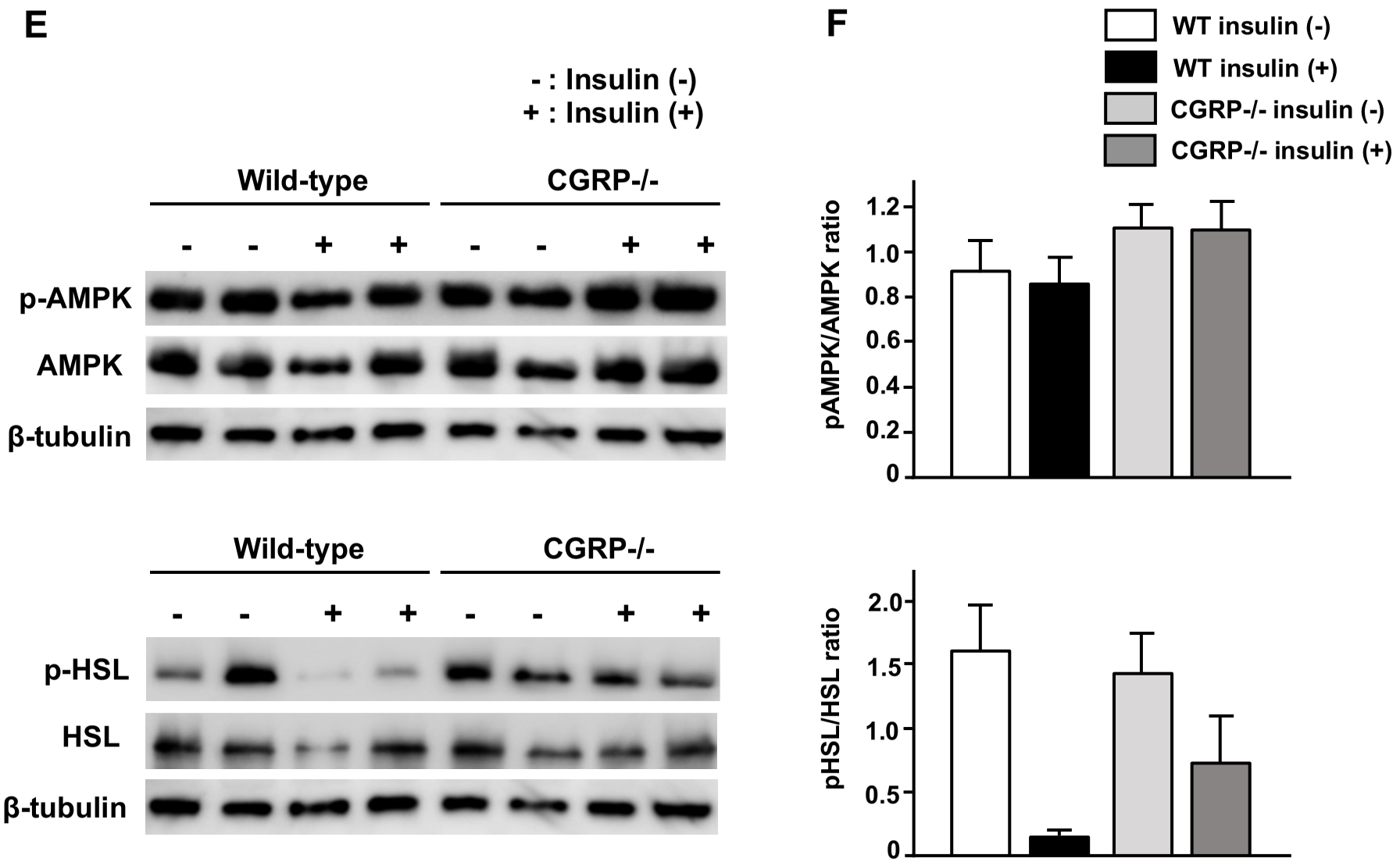
E
- : Insulin (-)
+ : Insulin (+)
Wild-type
CGRP-/-
- - + + - - + +
p-AMPK
AMPK
β-tubulin
Wild-type
CGRP-/-
- - + + - - + +
p-HSL
HSL
β-tubulin
F
WT insulin (-)
WT insulin (+)
CGRP-/- insulin (-)
CGRP-/- insulin (+)
pAMPK/AMPK ratio
0
0.2
0.4
0.6
0.8
1.0
1.2
pHSL/HSL ratio
0
0.5
1.0
1.5
2.0

Figure 6

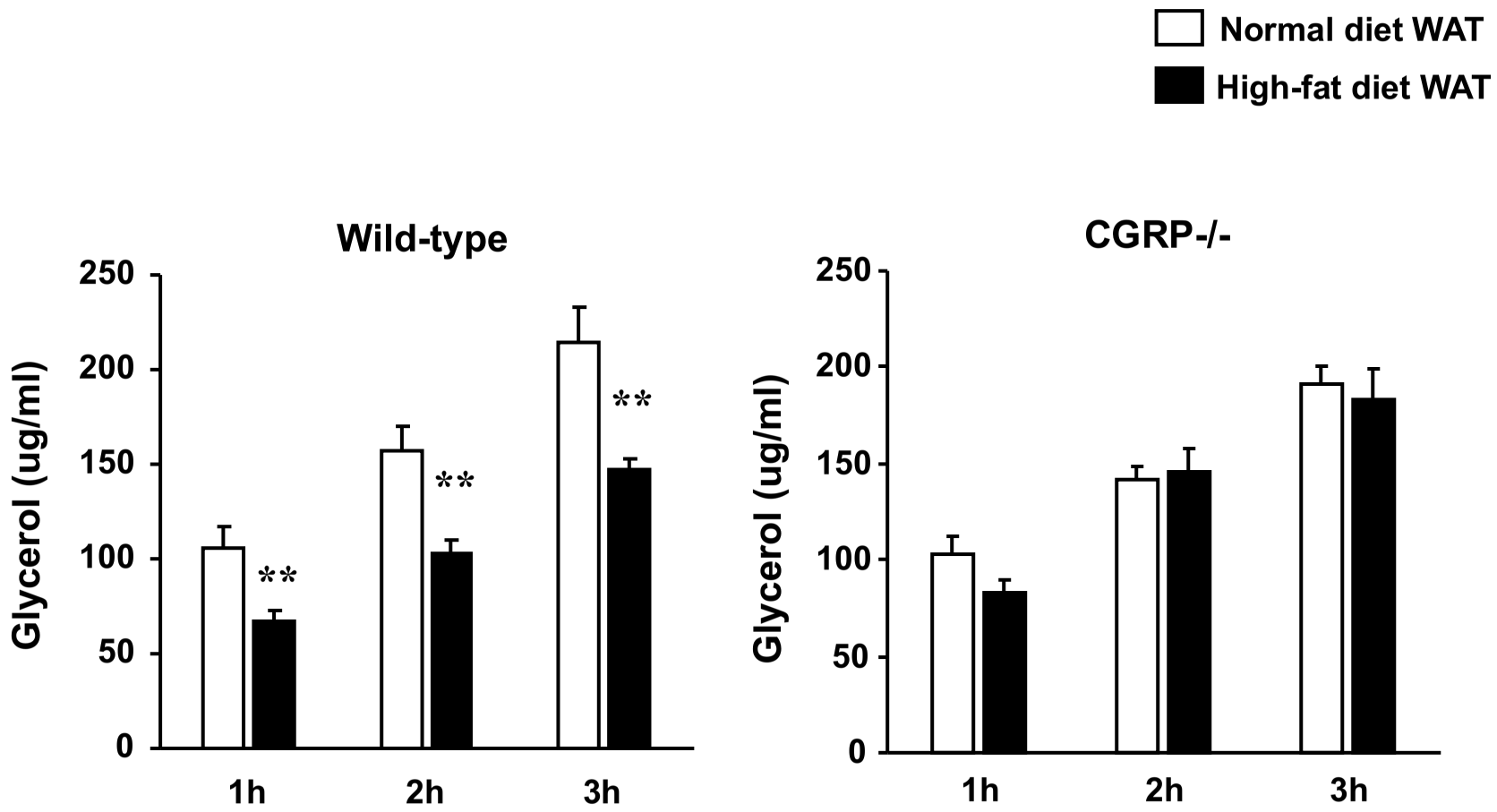
Normal diet WAT
High-fat diet WAT
Wild-type
CGRP-/-
Glycerol (ug/ml)
250
200
150
100
50
0
1h
2h
3h
**
**
**

Figure 7

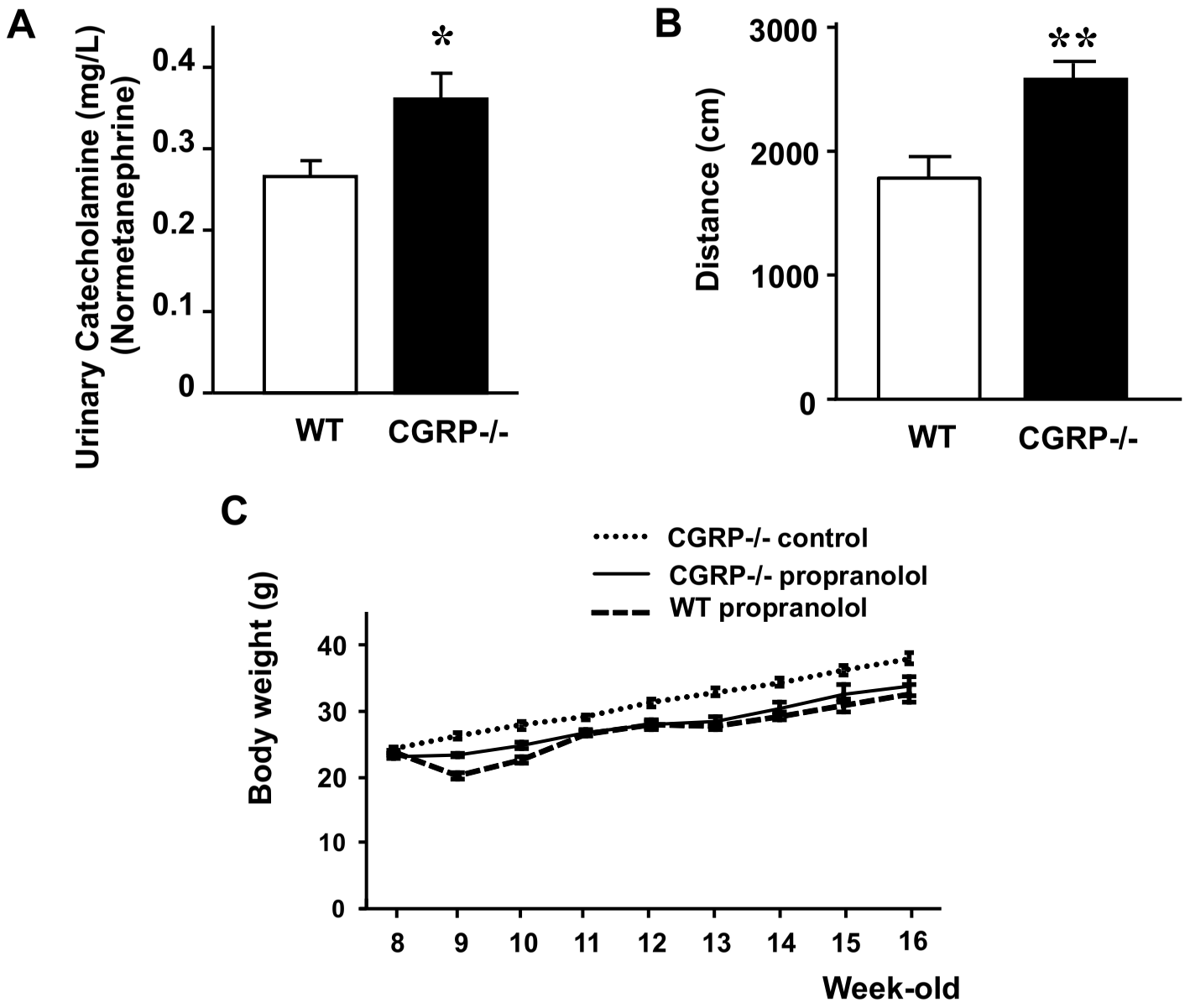
A
Urinary Catecholamine (mg/L)
(Normetanephrine)
0.4
0.3
0.2
0.1
0
*
WT
CGRP-/-
B
Distance (cm)
3000
2000
1000
0
**
WT
CGRP-/-
C
CGRP-/- control
CGRP-/- propranolol
WT propranolol
Body weight (g)
40
30
20
10
0
8
9
10
11
12
13
14
15
16
Week-old

Figure 8

Supplementary Figure Legends

Supplementary Figure 1. Corrected energy expenditure (data of **Figure 3H**) by grams of lean mass. All values are expressed as the mean ± SEM.**P<0.01 vs. WT.

Supplementary Figure 2. Analysis of glucose metabolism in WT and CGRP-/- mice after 10 weeks on a normal diet. **A, B,** Mice were subjected to oral glucose tolerance tests (OGTT) (**A**) and insulin tolerance tests (ITT) (**B**). For OGTT, 1 g/kg glucose was administered after fasting 16 h. For ITT, 1.5 U/kg insulin was intraperitoneally injected after fasting for 2 h. n = 5 in each group. All values are expressed as the mean ± SEM.

Supplementary Figure 3. Expression of genes associated with lipolysis (A), adiponectin (B) and adipocyte differentiation (C), as well as mitochondria-related genes (D) in WAT from mice on a normal diet. Expression levels in CGRP-/- mice were normalized to WT, which was assigned a value of 1. β3AR: β3-adrenergic receptor, HSL: hormone-sensitive lipase, CGI-58: comparative gene identification-58, AdPLA2: adipose phospholipase A2, PPAR: peroxisome proliferator activated receptor, TFAM: mitochondrial transcription factor A, ERRα: estrogen related receptor alpha, COX IV: cytochrome C oxidase, UCP: uncoupling protein. Bars depict means ± SEM. Statistical significance was analyzed using unpaired Student's t test. n = 5 in each group. *P<0.05 vs. WT.

Supplementary Figure 4. A, Expression of brown adipose tissue (BAT) markers. WT

and CGRP-/- mice were fed a high-fat diet for 10 weeks and BAT was sampled for the gene expression study. n = 5 in each group. Expression levels in CGRP-/- were normalized to WT, which was assigned a value of 1. UCP1: uncoupling protein 1, PGC-1α : peroxisome proliferator-activated receptor gamma coactivator 1-alpha, CIDEA: Cell Death Inducing DFFA Like Effector A, PRDM16: PRD1-BF1-RIZ1 homologous domain containing 16, Cox7a1: cytochrome c oxidase subunit 7a1, D2: type 2 iodothyronine deiodinase. All values are expressed as the mean ± SEM.

B, Expression of beige-ing-related genes in white adipose tissue (WAT). WT and CGRP-/- mice were fed a high-fat diet for 10 weeks and WAT was sampled for the gene expression study. n = 5 in each group. Expression levels in CGRP-/- were normalized to WT, which was assigned a value of 1.

Supplementary Figure 5. Expired gas analysis in WT and CGRP-/- mice on high-fat diet with oral administration of a β blocker (propranolol) at 14 weeks-old. Oxygen consumption (VO_2) (**A**) and CO_2 production (VCO_2) (**B**) were compared between WT and CGRP-/- mice. Means of these parameters for all day and the light and dark portions of the day are shown. n = 4 in each group. All values are expressed as the mean ± SEM.

Supplementary Figure 6. Comparison of the gene expression in WAT from CGRP-/- and WT mice on the high-fat diet with oral administration of the β blocker for 10 weeks. **A-D,** Expression of genes associated with lipolysis (**A**), adiponectin (**B**), and adipocyte

differentiation (**C**), and mitochondria-related genes (**D**) in WAT. n = 5 in each group. Expression levels in CGRP-/- were normalized to WT, which was assigned a value of 1. All values are expressed as the mean ± SEM.

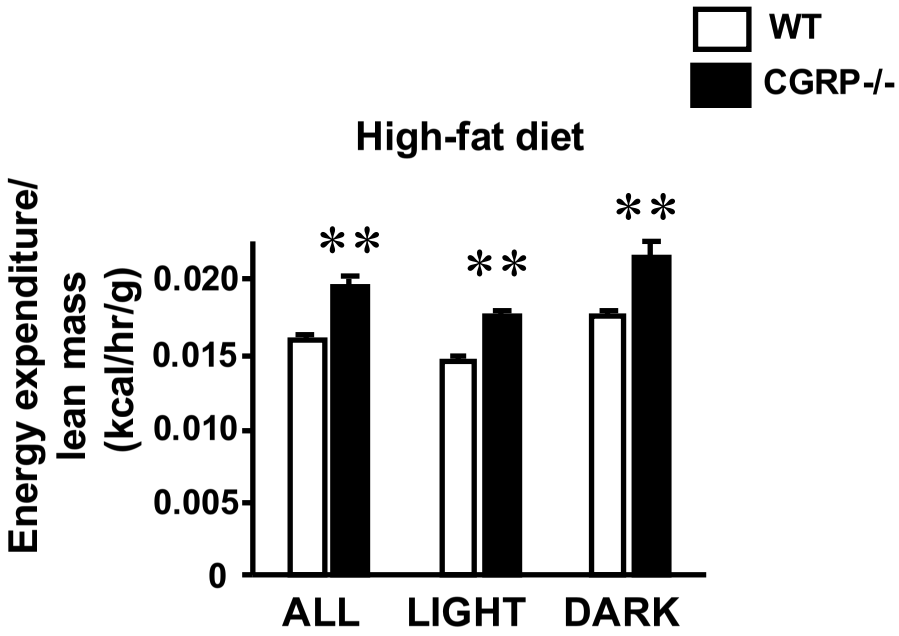

Supplementary Figure 1

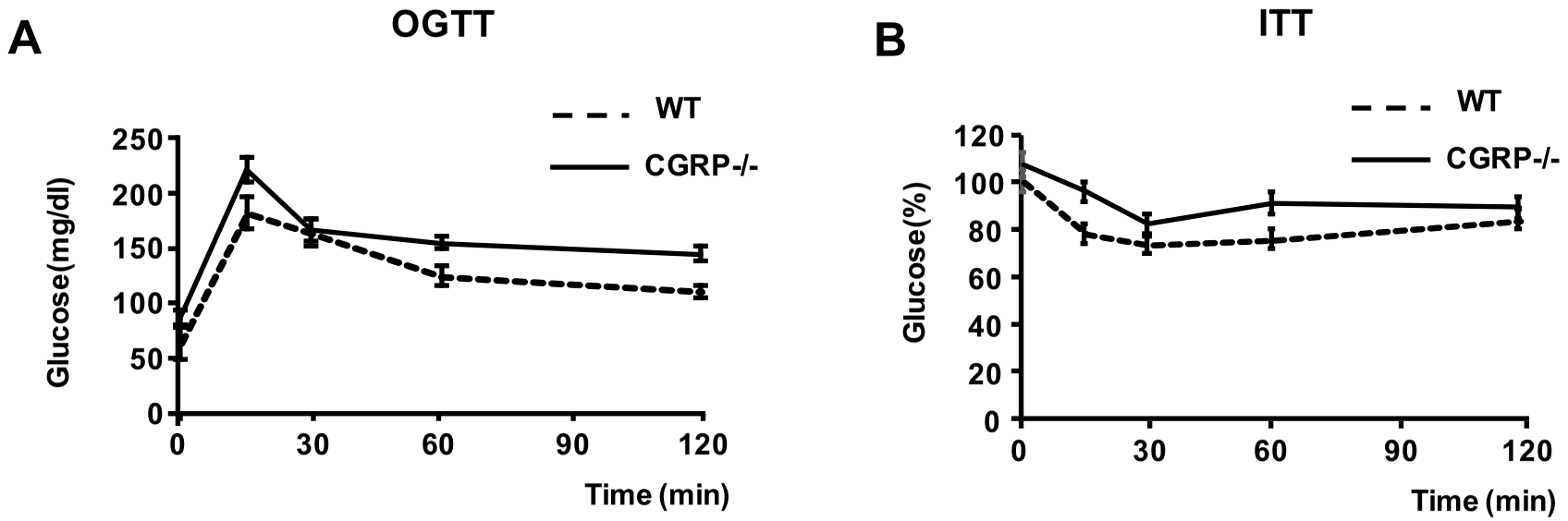

Supplementary Figure 2

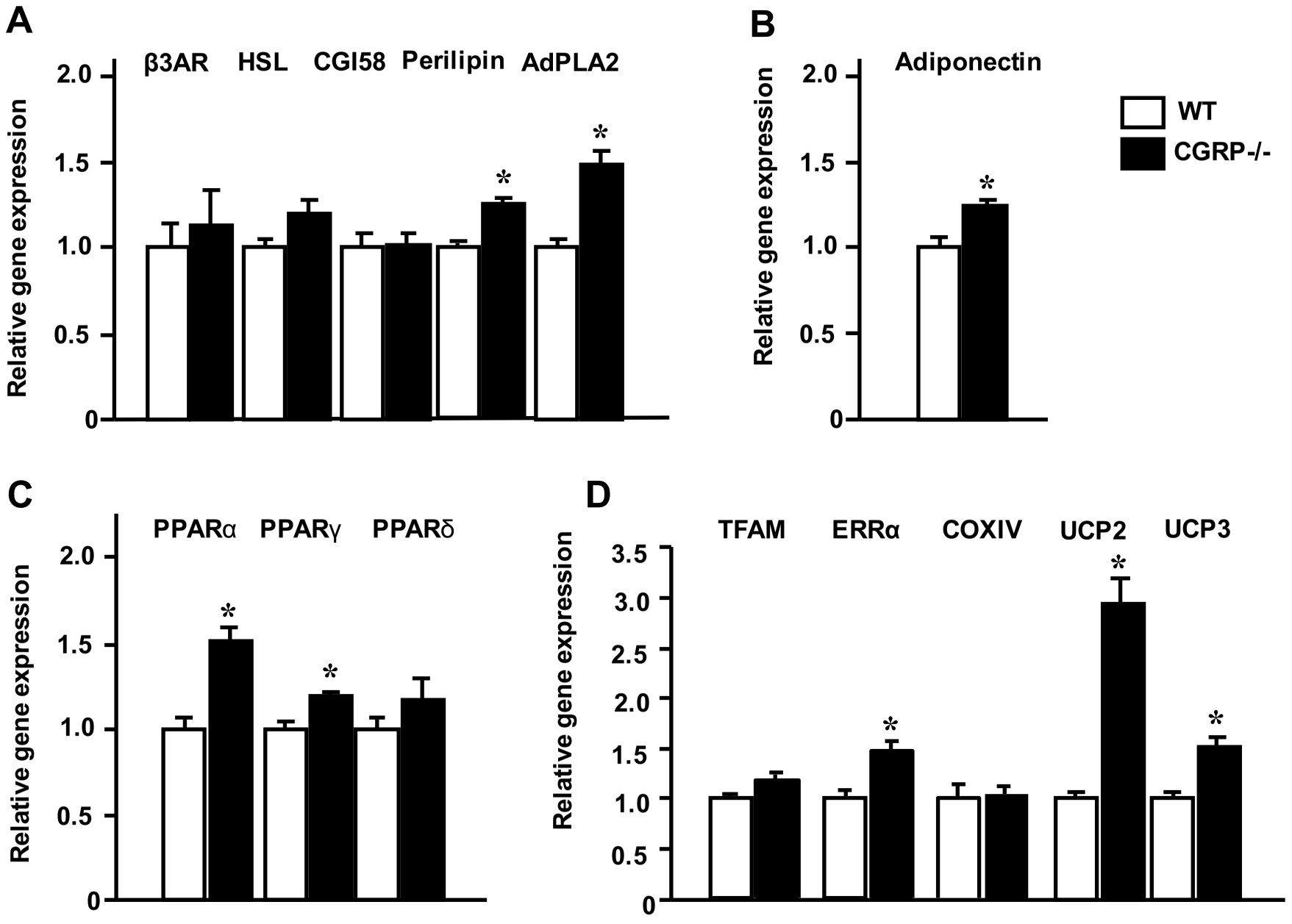

Supplementary Figure 3

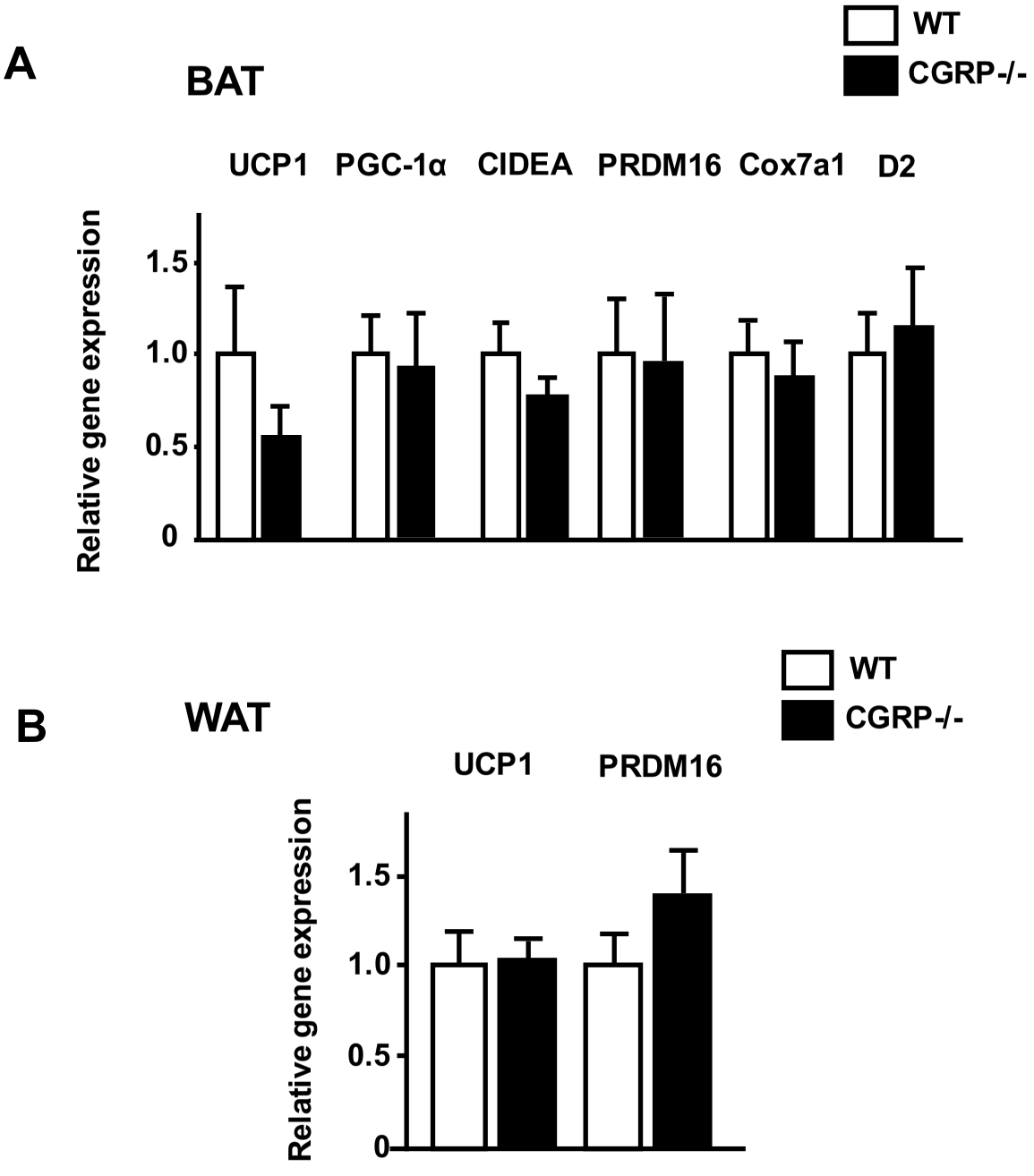

Supplementary Figure 4

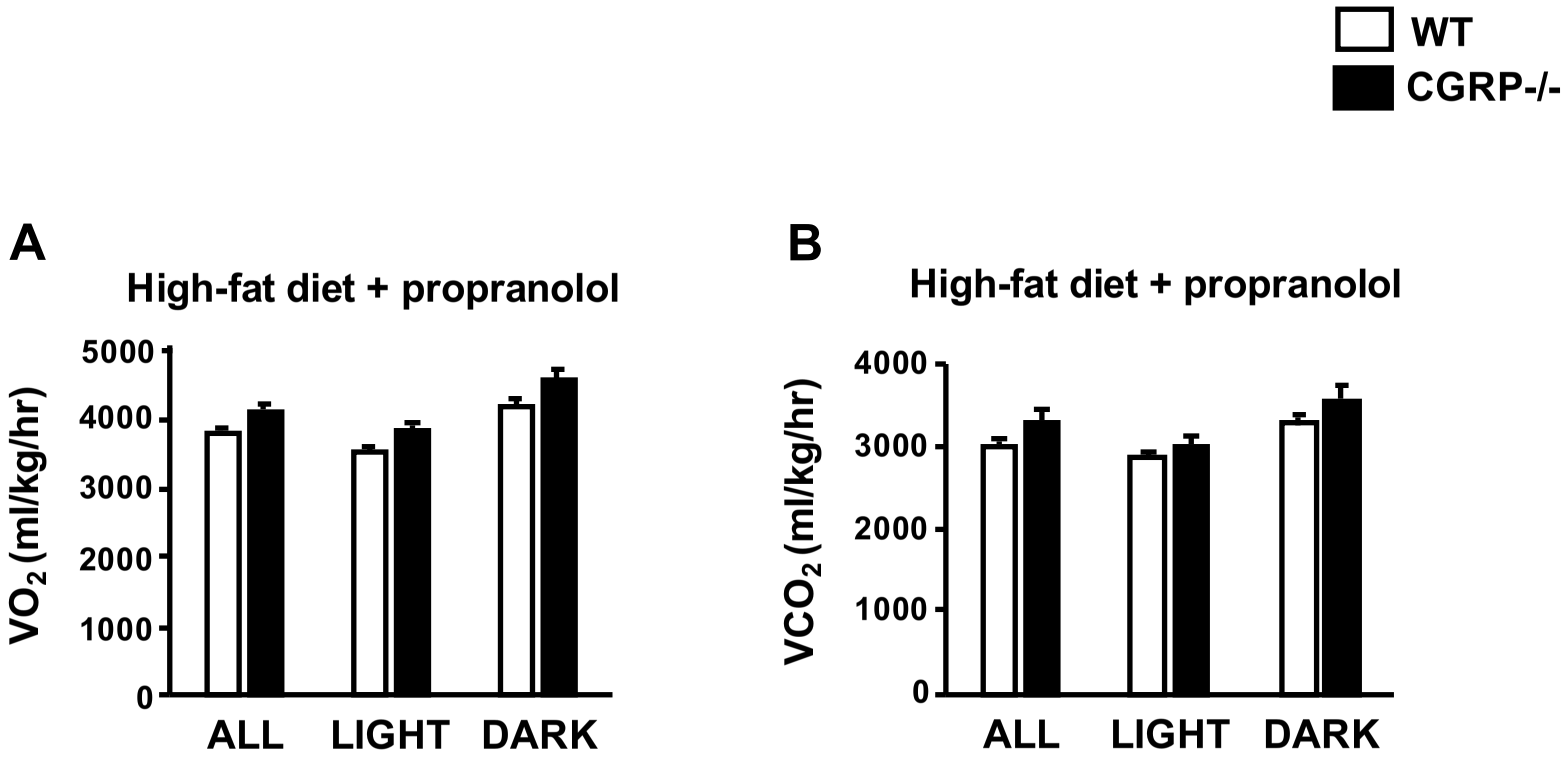

Supplementary Figure 5

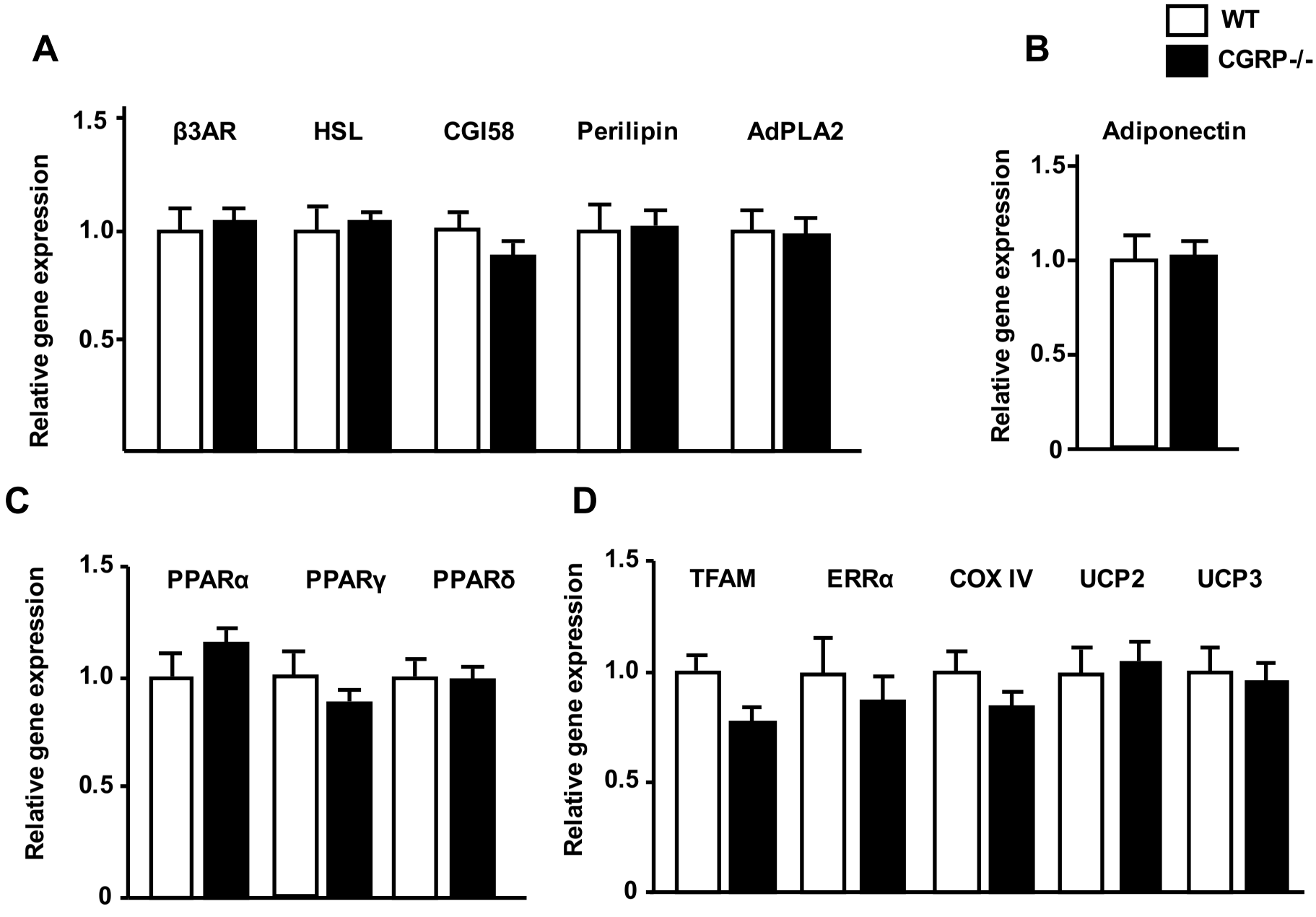

Supplementary Figure 6